



# CFD modelling of fire development in metro carriages under different ventilation conditions

Ying Zhen Li

BRANDFORSK Project 400-131

SP Technical Research Institute of Sweden

# CFD modelling of fire development in metro carriages under different ventilation conditions

Ying Zhen Li

## **Abstract**

### **CFD modelling of fire development in metro carriages under different ventilation conditions**

Fire development in a train carriage is investigated by CFD (Computational Fluid Dynamics) modelling. Two methods, i.e. the simple ignition model and the kinetic pyrolysis model, are applied. The model parameters are estimated and calibrated based on data obtained from small scale laboratory tests, including Thermo-Gravimetric Analysis (TGA) tests and cone calorimeter test carried out within the framework of the METRO project. Firstly, a full scale carriage fire test was simulated and the obtained results are compared with the test data. The comparison shows that both the simple ignition model and the kinetic pyrolysis model succeed to a large extent in predicting the fire development in the carriage. Further, the effects of ventilation and tunnel structure on fire development in carriages were investigated.

Key words: tunnel fire, metro carriage, fire development, ventilation, tunnel structure

**SP Sveriges Tekniska Forskningsinstitut**  
SP Technical Research Institute of Sweden

SP Report 2015:86  
ISBN 978-91-88349-05-7  
ISSN 0284-5172  
Borås 2015

# Contents

<b>Abstract</b>	<b>3</b>
<b>Contents</b>	<b>4</b>
<b>Preface</b>	<b>5</b>
<b>Summary</b>	<b>6</b>
<b>1 Introduction</b>	<b>8</b>
<b>2 State-of-the-art research</b>	<b>9</b>
2.1 Validation of FDS	9
2.2 Modeling of pyrolysis	9
2.3 Modeling of vehicle fires	10
2.4 Effect of ventilation and tunnel on fire development in carriages	10
<b>3 Theory of CFD modelling</b>	<b>12</b>
3.1 Pyrolysis modelling	12
3.2 Heat transfer in fuels	14
<b>4 Experiments</b>	<b>15</b>
4.1 Cone calorimeter tests	15
4.2 TGA tests	16
4.3 Full scale tunnel fire tests	16
<b>5 CFD modelling of small scale tests</b>	<b>20</b>
5.1 TGA tests	20
5.2 Cone calorimeter tests	22
<b>6 CFD modelling of full scale tunnel fire tests</b>	<b>26</b>
6.1 CFD model and parameters	26
6.1.1 Geometrical model	26
6.1.2 Boundary conditions	27
6.1.3 Fuels	27
6.2 Simulation with simple ignition model	30
6.3 Simulation with kinetic pyrolysis model	31
6.4 Short summary	32
<b>7 Effect of ventilation and tunnel structure</b>	<b>33</b>
7.1 Effect of tunnel structure	33
7.2 Effect of ventilation in well ventilated fires	35
7.2.1 Simple ignition model	35
7.2.2 Kinetic pyrolysis model	36
7.3 Effect of ventilation in vitiated fires under low ventilation	37
7.3.1 Heat release rates in vitiated fires	37
7.3.2 Vitiating under natural ventilation ( $u=0$ m/s)	39
7.3.3 Vitiating under low ventilation ( $u=1$ m/s)	41
7.4 Effect of ventilation in closely ventilation controlled fires	46
<b>8 Summary and conclusions</b>	<b>47</b>
<b>References</b>	<b>49</b>
<b>Appendix A - Yields of CO and smoke particles</b>	<b>51</b>

## **Preface**

This work was funded by the Swedish Fire Research Board (BRANDFORSK) which is greatly acknowledged. Thanks also to Prof. Haukur Ingason and Prof. Michael Försth at SP Fire Research for the valuable discussions and comments.

Test data used in this project were obtained within the framework of the METRO project. The author would like to acknowledge all the personnel and funders involved in these tests.

## Summary

Fire development in a train carriage is investigated by numerical simulations. Two methods, i.e. the simple ignition model and the kinetic pyrolysis model, are applied. The model parameters are estimated and calibrated based on data obtained from Thermo-Gravimetric Analysis (TGA) tests and cone calorimeter tests.

The first part of the work is to compare the simulated heat release rate curves with data from a full scale carriage fire test. The comparison shows that both the simple ignition model and the kinetic pyrolysis model succeed in predicting the fire development in the carriage to a large extent.

The simple ignition model predicts the heat release rate relatively well during the whole period with the only exception that the predicted fire growth rate is slightly lower than the test data. One possible reason is that the fire growth periods for different fuels were estimated from laboratory tests that could be longer than those in the full scale test where the radiation level inside the carriage is much higher. The maximum heat release rate is predicted well by the simple ignition model.

The kinetic pyrolysis model predicts the growth period well while the maximum heat release rate is much lower and the fire decays earlier. The energy content consumed in the simulation is also much lower than that in the test. These could be due to that some uncertainties could be introduced for the parameters obtained from small scale tests and there could be some fuels that are not accounted for. It is also found that the kinetic pyrolysis model is very sensitive to many parameters.

Overall, the simple ignition model could be deemed to perform better than the kinetic pyrolysis model in predicting the fire development in the carriage. However, for any simulation using these pyrolysis models, validation is always required, due to the sensitivity of these pyrolysis models to the input parameters, especially for the kinetic pyrolysis model.

The second part of the work is to investigate the effects of ventilation and tunnel structure on fire development in carriages.

The results show that for well ventilated carriage fires, e.g. when the longitudinal ventilation velocity is greater than around 1.5 m/s, the tunnel structure nearly has no effect on fire development in the carriage. The fire growth rate increases with ventilation while the maximum heat release rate is closely independent of the ventilation. For carriage fires under such conditions, the maximum heat release rate is approximately the same as that in a free-burn fire test in the open.

When the longitudinal ventilation velocity is not greater than a certain value (e.g. 1 m/s) and the reverse flow is arrested by the incoming flow (e.g. in a long tunnel), the fire could be highly vitiated. The fire develops more slowly and the maximum heat release rate becomes lower. We may call these fires as highly vitiated fires. For carriage fires under such conditions, the ratio of the maximum heat release rate to that in a well ventilated fire (or a free burn open fire) is around 0.6. The main reason should be that under such conditions, there exists a significant backlayering with a large amount of smoke, which is prevented by the incoming air flow and then blown back to the fire site, causing immediate smoke descend and vitiation of the fresh air at the fire site.

From the point of view of ventilation effect on the fire development, the distinction between the well ventilated fires and highly vitiated fires lies between 1 m/s and 1.5 m/s.

However, when the reverse flow is not arrested by the incoming flow in a tunnel, e.g. for a short tunnel or for a tunnel with no dominating ventilation (closely 0 m/s), the smoke could flow out of the tunnel through both portals. Under such conditions, there could be only a small portion of smoke is entrained into the incoming flow and blown back to the fire site. We may call these fires as lightly vitiated fires. The vitiation effect, therefore, depends on the tunnel length and the fire location relative to the portals. For a carriage fire in the middle of an approximately 100 m long tunnel, the ratio of the maximum heat release rate to that in a well ventilated fire (or a free burn open fire) is around 0.9. This ratio is expected to be slightly lower for a longer tunnel, but could not be lower than 0.6 which corresponds to highly vitiated fires.

If the fire size is smaller, both the amount of oxygen consumed and the mass flow rate of the reverse flow are reduced, which indicates less significant effect of vitiation on the fire development. Under such conditions, the transition point between well ventilated and vitiated fires could also be lower.

For all the cases, the effect of tunnel walls nearly has no effect on fire development in the carriage. Therefore the effect of heat feedback from tunnel structure is negligible for carriage fires. This is mainly due to the fact that the fuels in a carriage are not directly exposed to the tunnel structure.

It should be kept in mind that all the carriage fires discussed in this work are fuel controlled, despite the fact that inside the carriage the fire could closely be ventilation controlled to some extent, i.e. local flashover. In contrast, some large fires, e.g. tanker fires, could be closely ventilation controlled (fuel rich), that is, the heat release rate is directly related to the fresh air flows that are entrained into the fire site.

# 1 Introduction

Design fires have great influences on the fire safety concepts and safety measures, and are the basis for any assessment and calculation in tunnel fire safety design [1]. A design fire provides input data for the evaluation of thermal and toxic threat to evacuees, fire fighters as well as damage to structures.

At present, a widely used method is to classify design fires simply based on vehicle type, for example, a bus fire produces a heat release rate (HRR) of 20 to 30 MW fire, and a heavy goods vehicle (HGV) fire produces a HRR of 70 to 200 MW, according to NFPA 502 [2]. These data are generally obtained from large-scale or full scale fire tests.

Another widely used method is to directly use a fire curve from a full scale fire test as design fires, e.g. the Brunsberg tunnel fire tests carried out in 2011[3]. The heat release rate curves obtained from the full scale fire tests are valuable. However, a carriage could have different geometries, different openings and different internal materials. Therefore, the heat release rates obtained from limited full scale tests are not generically applicable as design fire curves for other carriages, although this is the common practice today. In summary, these widely used methods suggest that one vehicle type produces one fire size or one design fire curve, which is clearly not reasonable in practice. This also indicates that according to the present design guideline, no benefit in design fires could be obtained after using fire retardant materials in carriages, although use of fire retardant materials could delay a fire growth and lower a fire size.

The best way to obtain a design fire for a specific carriage is to carry out full scale carriage fire tests. However, the costs of such tests are huge and the number of the tests is typically limited.

CFD (computational fluid dynamics) modeling could be a good alternative to reduce the cost and make parametric studies possible after the model has been verified and adequately validated. This work uses a CFD tool to model the fire development in carriages based on data obtained from small scale laboratory tests. Within the framework of the METRO project [3], both full scale test data and laboratory scale material tests have been carried out. The data available through this project makes the present study possible. Data obtained from a large number of laboratory scale material tests will be used in the modeling. These small scale tests include Thermo-Gravimetric Analysis (TGA) tests and cone calorimeter test.

Another issue that needs to be addressed is the gap in knowledge on the effect of ventilation and tunnel structure on the design fires. There is much literature available arguing that the ventilation has huge influence on the heat release rate (see for example [4, 5]). However, given that for vehicle fires, most of the fuels are shielded and the fires are generally well ventilated in tunnels with longitudinal ventilation, the effect of ventilation on the heat release rate should be very limited. Further, for pool fires, most of test data used to support the viewpoint of large influence of ventilation on heat release rate come from small scale pool fires. It is well known that the heat release rate in a pool fire is strongly related to the flow pattern. For small pool fires the convective heat transfer is one key mechanism for mass burning rate. Increase of the ventilation passing through a small pool fire forces the flow pattern to change from laminar to turbulent flows which increases the convective heat transfer and burning rate. However, for large pool fires, an increase of ventilation will not significantly change the flow pattern and thus its influence on the heat release rate should be very limited. This issue needs to be clarified, however, such a parametrical study by full scale testing is costly. Rather, CFD calculations could be the only viable solution (provided the model has been verified).

## 2 State-of-the-art research

This section is divided into four parts: general validation of FDS (Fire Dynamics Simulator developed by NIST and VTT [6, 7]), modeling of pyrolysis, CFD modeling of carriage fires, and effects of ventilation and tunnel structure on fire development in carriages.

### 2.1 Validation of FDS

There are three methods to simulate the burning of solid fuels in FDS: gas burner with a specified heat release rate per unit area (the HRRPUA model), solid fuels that burn at a specified rate with ignition temperature (the simple ignition model) and solid fuels that burn following the Arrhenius pyrolysis model (the kinetic pyrolysis model).

FDS has been validated in many scenarios. Generally, good agreement between the FDS results and experimental data can be obtained if the work focuses on prediction of gas temperatures, smoke and flows based on the HRRPUA model, i.e. pre-described fire. For example, Ma and Quintiere [8] studied axi-symmetric fire plumes comparing predicted flame heights and plume centre line temperatures to both empirical correlations and experimental data. Good agreement occurred in the far field plume region except for very coarse grids and reasonable grid size was proposed for modeling of the free fire plume. Li et al. [9] carried out FDS simulations of the Runehamar tunnel fire test T1 and the FDS results correlated well with the tests data for gas temperatures, heat fluxes, except in far-field downstream where a slight overestimation was found.

However, worse correlation has been obtained concerning modeling fire development, using the simple ignition model and the kinetic pyrolysis model. For example, NIST compared simulations and experiments for a fire involving three office work stations in a compartment, to validate FDS for use in the world trade center investigation [10]. Burning parameters for some materials such as desks, partitions and carpet were defined using the simple ignition model and other materials such as boxes and papers were defined using the HRRPUA model. Peak heat release rate and temperatures were predicted to be within 20% for all tests although significant deviations in the time and trends for HRR and temperature curves were found.

In summary, the simple ignition model and the kinetic pyrolysis model used to model the fire development are still being developed and need verification and sensitivity analysis of their capability before they can be used to reliably predict any fire scenario. Further, small scale test data are necessary as input for this type of modeling and such data is seldom available in sufficient detail.

### 2.2 Modeling of pyrolysis

There has already been a long history of modeling of pyrolysis in fire community. In the 1980's, Parker [11] built on a heat release rate prediction model based on the mass loss rate model of Atreya [12]. The basic concept is to assume a one dimensional heat transfer process to calculate the fuel temperature and to use a Arrhenius type equation to estimate the pyrolysis rate. Their theoretical models are still used today.

The main difficulty in practical applications is to obtain the pyrolysis kinetic properties and thermal properties. Detailed measurements are required. Moreover, many of the

properties are not really physical properties but more experimental constants. Further, the properties mostly vary with temperature. A comparison of the model implemented and the properties used with experimental data is always required before any practical application.

In reality, at this stage, extensive researches are carried out on modeling of pyrolysis process of some single samples and/or trying to obtain their kinetic properties by use of Thermo-Gravimetric Analysis (TGA), Micro-Combustion Calorimetry (MCC) and Fire Propagation Apparatus (FPA) [13]. Pau et al. [14] investigated different analytical methods to determine the kinetic properties of pyrolysis of a non-fire-retardant and a fire retardant polyurethane foam with TGA tests. Matala et al. [15] introduced a new analytical direct method. Curve-fitting algorithms have also been used for estimation of the pyrolysis kinetic properties, including the generic algorithms (GA) (see for examples Rei et al [16] and Matala et al. [17]), hybrid genetic algorithms (HGA) [18] and shuffled complex evolution (SCE) [13].

There is a lack of CFD studies on pyrolysis modeling of large scale fire tests, especially for complex fuel configurations.

## **2.3 Modeling of vehicle fires**

Quite limited work has been conducted on the CFD modeling of vehicle fires. Kit [19] carried out an FDS study to simulate the fire development of an SP pallet test and Runehemar test [20] based on a series of simplifications of the burning objects and small scale tests data obtained from the literature. The maximum heat release rate was predicted fairly well but not the fire curve. White [21] reported the CFD work done in 2006 by fire engineering students at Worcester Polytechnic Institute using an old version FDS (FDS4) to obtain an estimation of the HRR curve in a half train carriage fire. The results did not show good correlation and it was pointed out that inputs of appropriate material properties for combustible materials and glazing were probably the most significant source of error. Hjøhlman et al. [22] simulated a train compartment fire and obtained relatively good results, however, the train compartment studied was a small confined compartment consisting of only 4 seats and thus is not representative of commonly used carriages. Guillaume et al. [23] simulated full scale train carriage fires using FDS5 in the Transfeu project. However, the fire did not really spread and thus the heat release rate mainly originated from the ignition source, i.e. the gas burner placed beside the seat.

## **2.4 Effect of ventilation and tunnel on fire development in carriages**

Carvel et al. [4, 5] carried out probability studies on the effect of ventilation and tunnel structure on the heat release rate in tunnel fires and concluded that the ventilation and tunnel structure could have a huge influence on the heat release rates, and the ratio of heat release rate in a tunnel to that in the open could be up to 10. However, the conclusions are questionable. The input data for their probability model were empirical and many tests data came from small scale pool fire tests.

From our previous studies [24-27], it was concluded that for well ventilated vehicle fires with the main fuels exposed to ventilation flows, the ventilation mainly influences the fire growth rate and has an insignificant effect on the maximum heat release rate. Under very

low ventilation conditions, the heat release rate could be slightly lower than that in the free-burn test.

In a vehicle fire with fuels not directly exposed to ventilation flows, e.g. in a metro carriage which is partly enclosed only with the doors open for evacuation and the windows broken when exposed high heat fluxes, the influence of ventilation on the fire development was found to be even less. However, how much the ventilation conditions may affect the fire development is not clear and needs to be clarified in this specific scenario.

### 3 Theory of CFD modelling

The Fire Dynamics Simulators (FDS) is widely used in the fire community [6, 7] and has become a standard of fire modeling. The latest version FDS6 is used in this project. In the following, a short description of the pyrolysis model and heat transfer model is given.

#### 3.1 Pyrolysis modelling

As mentioned previously, there are three methods to simulate the burning of solid fuels in FDS:

*HRRPUA model:* Gas burner with a specified heat release rate per unit area (HRRPUA).

*Simple ignition model:* Solid fuels that burn at a specified rate (Ignition temperature).

*Kinetic pyrolysis model:* Solid fuels that do not burn at a specified rate (Arrhenius kinetic pyrolysis).

Note that the HRRPUA model is not suitable for estimation of fire development since it pre-describes the fire curve rather than estimating it by modeling. Only the simple ignition model and the kinetic pyrolysis model could be used in the project based on data from different test series.

In the simple ignition model, an ignition temperature is assigned to a combustible material which burns only after the surface temperature reaches the ignition temperature. After ignition, the fuel burning also follows the prescribed HRRPUA.

In the kinetic pyrolysis model, the kinetic parameters of the reactions specified for each material are used to describe the reactions that occur within the solid materials while they are burning.

In this work, the simple ignition model and the kinetic pyrolysis model are applied to simulate the burning of the fuels as the main purpose is to predict the heat release rate rather than prescribe it. In the following, the theory related to the kinetic pyrolysis model is discussed in more detail.

In case of a fire, solid fuels mostly undergoes a chemical decomposition process, i.e. pyrolysis, that produce combustible volatiles for gas phase combustion (flaming combustion). This process is mostly endothermic, but it may accompany oxidation that releases heat, e.g. in case of a smouldering fire.

The rate of pyrolysis, or reaction rate, is widely expressed using the Arrhenius equation in such a form:

$$r = -\frac{dY}{dt} = AY^n \exp\left(-\frac{E}{RT}\right) \quad (1)$$

where  $Y$  is mass fraction (kg/kg),  $n$  is reaction order,  $t$  is time (s),  $A$  is pre-exponential coefficient (1/s),  $E$  is activation energy (kJ/kmol),  $R$  is universal gas constant (kJ/(kmol·K)) and  $T$  is absolute gas temperature (K).

The Arrhenius equation is an approximate form of the pyrolysis rate. In most cases, the parameters including pre-exponential coefficient, activation energy and reaction order, need to be determined from experimental data. In this work it is assumed that each fuel consists of several components and each component undergoes a first order reaction. The pyrolysis rate is therefore the sum of multiple components for a specific fuel type.

Small scale tests such as Thermo-Gravimetric Analysis (TGA) and Micro-Combustion Calorimetry (MCC) tests could be carried out to obtain these required information. Thermo-Gravimetric Analysis (TGA) equipment measures the mass of the sample exposed to a continually increasing temperature in either an inertial environment (nitrogen, helium), or under oxygen conditions (normal or some other certain percentages). The most two common test conditions are in nitrogen or air. The increasing temperature rate could vary from 2 K/min to 60 K/min. Micro-Combustion Calorimetry (MCC) equipment follows a similar test procedure but the pyrolysis gases are burned in a hot environment before exiting the equipment. The heat released is estimated by the oxygen consumption technique.

The reaction could be assumed to be first order, that is,  $n=1$ . The pre-exponential coefficient, A, can then be obtained from TGA test data [28]:

$$A = \frac{er_p}{Y_0} \exp\left(\frac{E}{RT}\right) \quad (2)$$

where e is natural exponential coefficient,  $r_p$  is the peak value of pyrolysis rate and  $Y_0$  is the initial mass fraction (kg/kg).

The activation energy E can obtained by [28]:

$$E = \frac{er_p RT^2}{Y_0 (dT / dt)} \quad (3)$$

where  $dT/dt$  is the TGA temperature increasing rate (K/s).

These two equations correlate the test data with the key parameters.

If there is residue left as it is in most cases, the following equation is introduced to correlate the assumed mass fraction and the realistic mass fraction in a TGA test:

$$\frac{dY}{dt} = \frac{1}{1 - Y_{0,r}} \frac{dY_{TGA}}{dt} \quad (4)$$

where  $Y_{0,r}$  is the residual mass fraction of the original fuel (kg/kg).

A fuel could consist of several components and each component undergoes its own reaction. Therefore, the overall reaction rate is the sum of the individual parts.

In FDS simulations, the oxidation process could also be simulated. The equation for the reaction rate could be modified to:

$$r = -\frac{dY}{dt} = AY^n \exp\left(-\frac{E}{RT}\right) (X_{O_2}(x))^{n_{O_2}} \quad (5)$$

where  $n_{O_2}$  is the oxygen reaction order, which is zero by default. The oxygen concentration inside a solid is estimated from the nearest gas on the surface:

$$X_{O_2}(x) = X_{O_2,g} \exp(-x / L_{ox}) \quad (6)$$

where  $x$  is depth below surface, and  $L_{ox}$  is characteristic depth of oxygen diffusion. Subscript  $g$  indicates gas phase nearby the surface. The oxidation is not considered in this work.

## 3.2 Heat transfer in fuels

The heat conduction inside fuels or structure is simplified into one-dimensional problem and its controlling equation can be expressed as:

$$\rho_s c_s \frac{\partial T_s}{\partial t} = \frac{\partial}{\partial z} (k_s \frac{\partial T_s}{\partial z}) + \dot{q}_s'' \quad (7)$$

with the boundary on the surface exposed to gas:

$$-k_s \frac{\partial T_s}{\partial z} = \dot{q}_{w,c}'' + \dot{q}_{w,r}'' \quad (8)$$

where  $k$  is the conductivity (kW/mK),  $\rho$  is density (kg/m<sup>3</sup>),  $c$  is heat capacity (kJ/(kg·K)),  $T$  is the temperature (K),  $z$  is the vertical distance from the surface (m),  $\dot{q}_s''$  is the heat production or loss rate which mainly comes from chemical reactions, and  $\dot{q}_w''$  is the absorbed heat flux on the wall surface. Subscript  $s$  means solid,  $w$  means wall,  $c$  means convective and  $r$  means radiative.

## 4 Experiments

Within the framework of the METRO project [3], a series of tests were carried out, including cone calorimeter tests, TGA tests and full scale fire tests.

### 4.1 Cone calorimeter tests

Cone calorimeter [29] is a standard test facility to measure burning behaviors of different fuels, see Figure 1. The basic parameters such as HRR, CO and soot production obtained from cone calorimeter tests could be used in CFD simulations.

The fuels tested in cone calorimeter include the floor, the wall and the seat, with an exposed heat flux of 25 kW/m<sup>2</sup>, 50 kW/m<sup>2</sup>, and 25 kW/m<sup>2</sup> respectively. For each sample, two tests were carried out, i.e. one test and one repeat test.

The fuel samples were tested according to their configurations in the full scale carriage. The floor has two layers, i.e. a layer consisting of 12 mm thick plywood with a 2 mm thick PVC cover, and a layer of 9 mm thick styrofoam beneath. The wall and ceiling linings consisted of two layers, i.e. 3 mm thick high pressure laminate (HPL) and 18 mm thick low density plastic. The seat consists of 2.4 mm thick fabric, 10 mm thick polyurethane foam and 15 mm thick wood board.



Figure 1 Cone calorimeter test for one seat material in the METRO project.

The soot and CO yields are estimated according to the theoretical model presented in Appendix A. The results are given in Table 1. The transient values are estimated based on the mass flow rate while the global values based on the mass. Both soot and CO yields vary significantly during the tests. In the simulations, the average global values estimated based on mass are used.

Table 1 Soot yield and CO yield for the fuels in the cone calorimeter test.

Fuel type	Exposed heat flux	Transient value*		Global value**	
		$Y_{soot}$	$Y_{CO}$	$Y_{soot}$	$Y_{CO}$
	kW/m <sup>2</sup>	kg/kg	kg/kg	kg/kg	kg/kg
Wall	50	0.006-0.05	0.05-0.15	0.011	0.144
Floor	25	0.02-0.1	0.05-0.10	0.029	0.07
Seat	25	0.01-0.08	0.05-0.10	0.017	0.062

\* based on mass flow rate. \*\* based on total mass.

## 4.2 TGA tests

TGA tests have been carried out to obtain the detailed kinetic properties. In the tests, the ambient temperatures were increased gradually and the mass loss was measured. The fuels tested in TGA tests include the floor, floor insulation, wall, wall insulation and seat. The samples were very small and not cut into very fine pieces.

Figure 2 shows the TGA test data for the seat in the C20 metro carriage. The X axis is the surrounding temperature and Y axis is the mass fraction. Two series of tests have been done, one with ambient air and temperature increase of 20 °C per minute, and another with N<sub>2</sub> atmosphere and 5 °C per minute. These data are required to be used as inputs into the Arrhenius kinetic pyrolysis model.

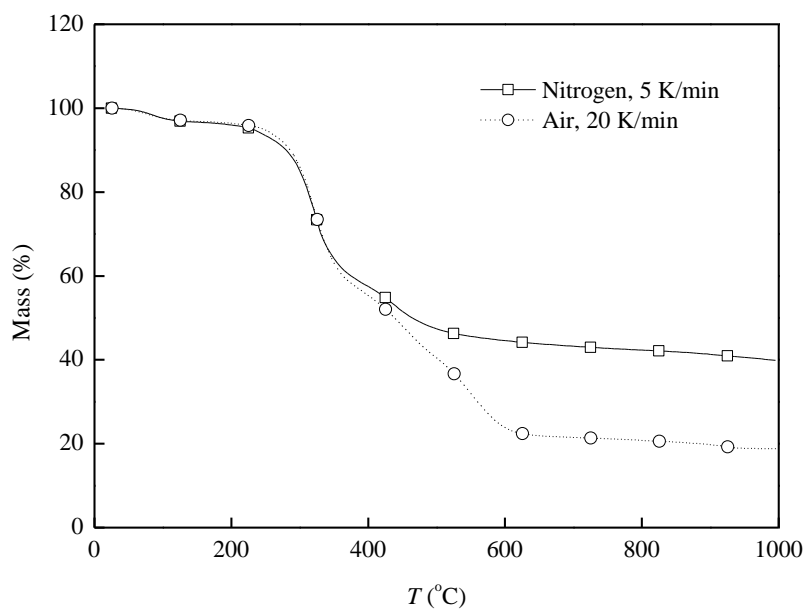


Figure 2 TGA tests for mass losses of the seats in the C20 metro carriage.

Data obtained from these laboratory tests will be used to adjust and validate the CFD modeling before carrying out the simulations of full scale carriage fires.

## 4.3 Full scale tunnel fire tests

Three full scale metro carriage fire tests were carried out in Brunsberg tunnel in 2011 to investigate fire development inside the metro carriages [3], see Figure 3. Data obtained from the full scale tests will be used for comparison with the fire curves obtained using CFD modeling after the CFD modeling has been adjusted and validated.



Figure 3 Brunsberg tunnel fire test in the METRO project (photo Per Rolén).

The tunnel is 276 m long and the carriage was positioned 96 m from the eastern tunnel entrance, see Figure 4. The tunnel air flow direction is from east to west.

The full scale tests were performed in the old Brunsberg tunnel, located between Kil and Arvika in western Sweden. This abandoned tunnel lies on a siding about 1 km long. It was taken out of service when a new tunnel was constructed close by to reduce the sharpness of a bend in the route.

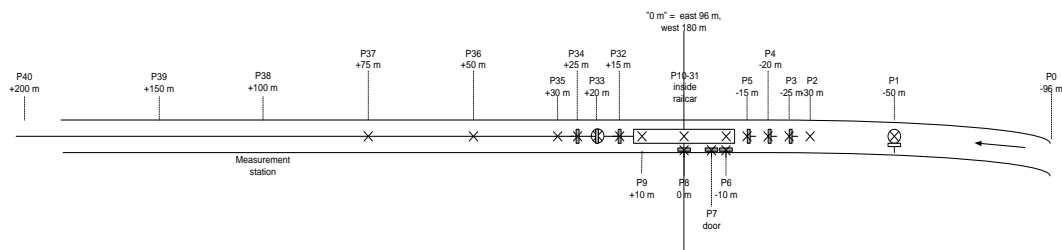


Figure 4 A diagram of the Brunsberg tunnel and the measurement points. Left corresponds to the west.

The cross-section of the tunnel varies along the tunnel and to obtain a better view of this variation, the cross-section was registered at 21 different positions along the tunnel. The tunnel height varied in these measurements between 6.7 m and 7.3 m with an average of 6.9 m. The width at the ground level varied between 5.9 m and 6.8 m with an average of 6.4 m. The cross section 100 m downstream is shown in Figure 5 with measurements.

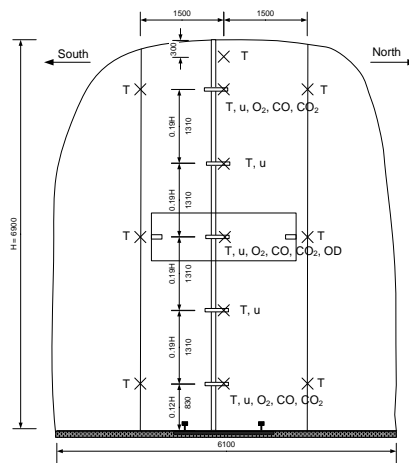


Figure 5 Cross-section of the Brunsberg tunnel and measurements at +100 m.

The train consists of a 22 m long carriage and a 2.6 long driver cabin, see Figure 6. In total three tests were carried out. In test 1, a heptane pool was placed underneath the railway carriage to evaluate the risk for fire spread to inside of the carriage. Test 2 and test 3 are carriage burning tests. In the first two tests, a X1 train was used. In test 3, a refurbished X1 train, simulating a modern C20 train, was used. The interior walls and ceilings were fully covered by aluminium and also some blocks beside the doors were installed. Furthermore, the seats were changed to more modern ones, see Figure 7.

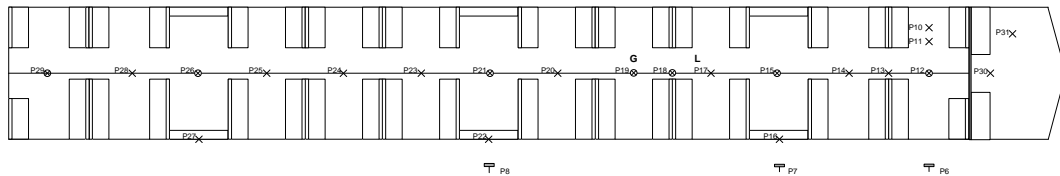


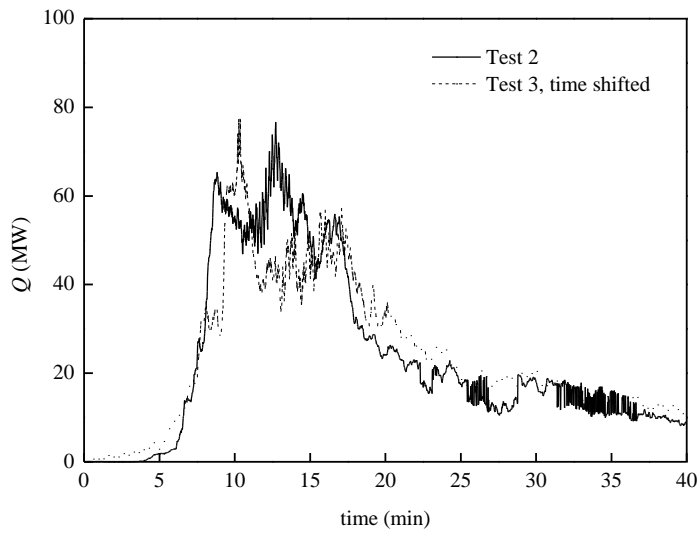
Figure 6 Instrumentation of the carriage.



Figure 7 Interior design of a X1 train and a refurbished X1 train (simulating the interior of a C20 train).

The total fire load of the train excluding the luggage and the driver cabin was estimated to be 35.4 GJ. The estimation is based on information on walls, ceiling, floor and seats. Cables, etc. are not included in the estimation. In total 79 pieces of luggage were used with an average mass of 4.44 kg and a total mass of 351 kg. If an average energy content of 25 MJ/kg is assumed the extra fire load corresponds to 8.8 GJ, which represents 20 % of the new total fire load (44.2 GJ).

Figure 8 shows the heat release rate in Test 2. In comparison, data for test 3 are also presented but with a time shift of 107 min. As mentioned previously, the delay of fire development was mainly due to the aluminium lining inside the carriage. Figure 8 show high similarity between the HRR curves in Test 2 and Test 3. Although the time to maximum HRR was delayed in Test 3, the main fire curve was approximately the same as that in Test 2. This phenomenon was also observed in model scale tests [30]. There are mainly two reasons for this. Firstly, the energy content consumed before the rapid growth stage was quite small, compared to the total energy consumed in the tests, about 10 % in Test 3. Secondly, the fully developed metro carriage fires are quite similar since at the stage the fire in the carriage is so-called “ventilation controlled”.



*Figure 8. Heat release rate curves in Test 2 and Test 3 (Modified time in Test 3).*

The full scale test 2 is simulated in this project, but not the full scale test 3. The main difference between these two tests is that in test 3 aluminium linings were applied to the walls and ceiling of the carriage. Note that under high temperatures the aluminium melts down, leaving fuels exposed to the hot gases. The uncertainty for simulating the test 3 is therefore much higher compared to test 2. Therefore only test 2 is simulated in this project.

## 5 CFD modelling of small scale tests

The main objective of this section is to estimate and calibrate the inputs for the kinetic pyrolysis model.

### 5.1 TGA tests

The TGA tests were simulated with the one dimensional model in FDS. The small samples were considered as thermally-thin materials with surfaces exposed to the prescribed linearly increasing temperatures. The main purpose is to check whether the pyrolysis rates obtained from TGA tests for different fuels can be well represented by the pyrolysis model in FDS.

Comparisons of test data and FDS results of the pyrolysis rate,  $dY/dt$ , for the floor and the floor insulation are shown in Figure 9 and Figure 10, respectively. Clearly, test data correlate well with the FDS results.

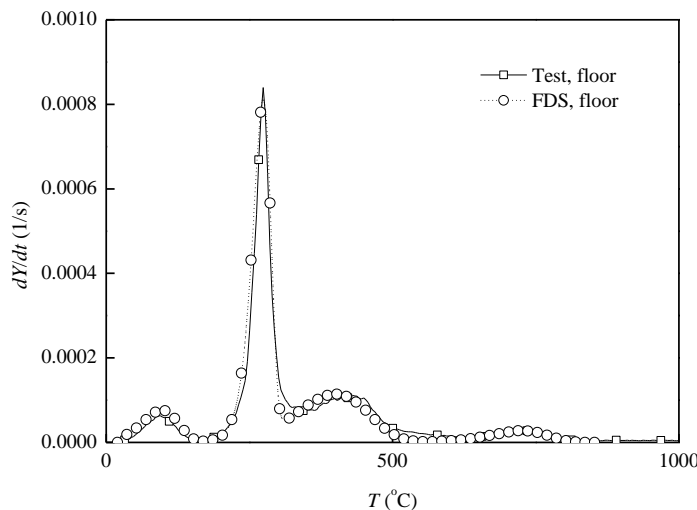


Figure 9 Comparison of FDS results and TGA test data for floor.

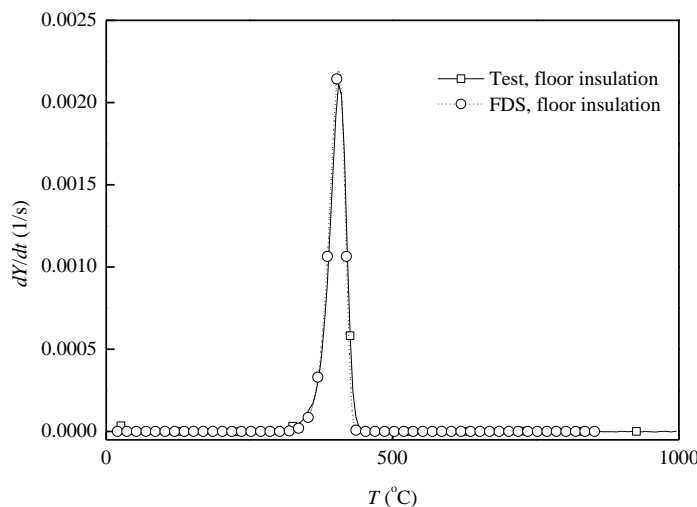
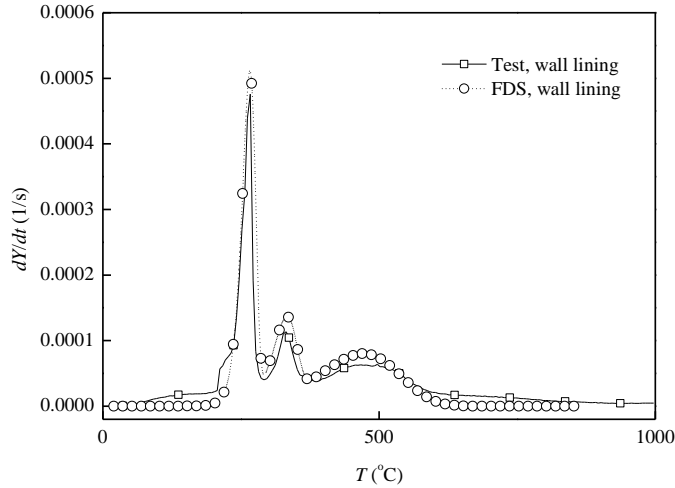
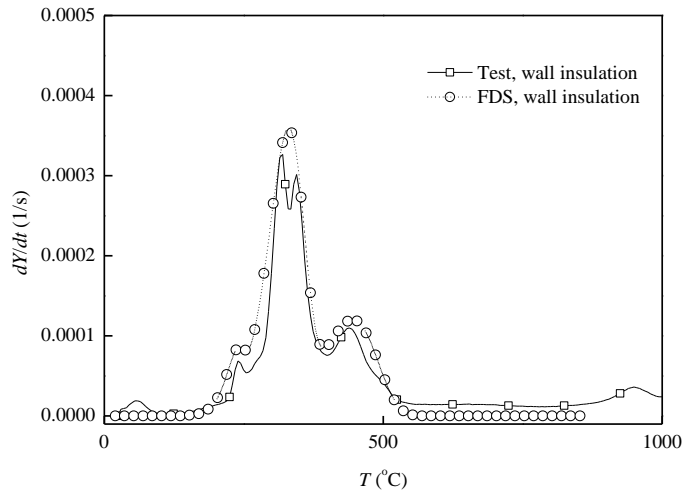


Figure 10 Comparison of FDS results and TGA test data for floor insulation.

Comparisons of test data and FDS results of the pyrolysis rate for the wall lining and wall insulation are shown in Figure 11 and Figure 12, respectively. Clearly, test data correlate well with the FDS results.



*Figure 11 Comparison of FDS results and TGA test data for wall lining.*



*Figure 12 Comparison of FDS results and TGA test data for wall insulation.*

Comparisons of test data and FDS results of the pyrolysis rate for the wall insulation is shown in Figure 13. It is clearly shown in Figure 13 that test data correlate well with the FDS results.

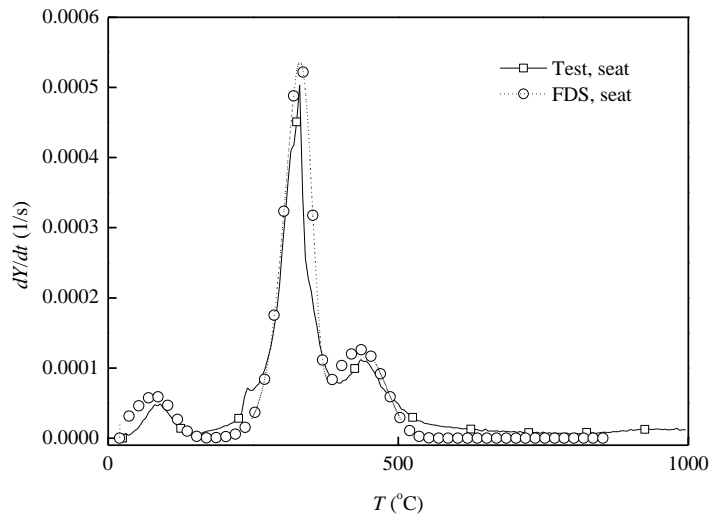


Figure 13 Comparison of FDS results and TGA test data for seat.

From the above analysis, it can be concluded that the pyrolysis rates obtained from TGA tests can be well represented by the pyrolysis model in FDS for the fuels considered here, including the floor, floor insulation, wall lining, wall insulation and seat. These pyrolysis models will then be used in simulations of the cone calorimeter tests in the following.

## 5.2 Cone calorimeter tests

The cone calorimeter tests is simulated with the TGA data as inputs. The CFD model for the cone calorimeter tests is shown in Figure 14. The computation domain is 0.2 m long, 0.2 m wide and 0.4 m high. Geometrical properties and density are measured while other thermal properties are obtained in the literature [31-33].

In order to simulate an imposed heat flux on the samples, fixed surface temperatures are set on the inner surfaces of the cone heaters (gray objects). Before the simulations, a series of trials was made to obtain a correlation table for the heater temperature and the incident heat flux on the sample bed. Distribution of heat fluxes on surfaces along the diagonal (green points in Figure 14) was found to be very uniform except the point close to the edge.

The actual incident heat flux consists of both this imposed external heat flux and the heat flux from the combustion flame above the sample. These two fluxes are mostly comparable and thus neither of them is negligible in the simulations of the cone calorimeter tests. Despite this, pre-simulations are carried out with a guessed net heat fluxes to roughly check the results, simply by turning off the heat transfer between the surface and gas. The results from these pre-simulations however are not presented here.

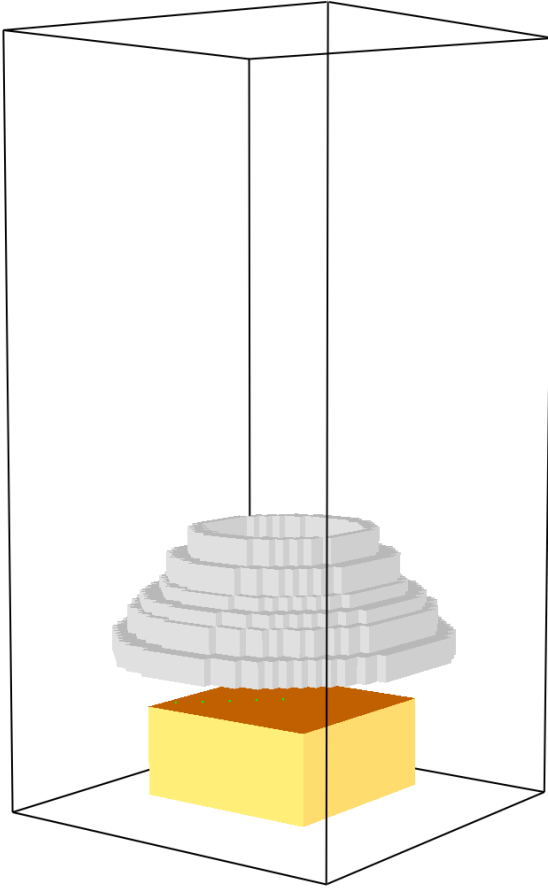


Figure 14 CFD model of the cone calorimeter tests.

The properties of the fire plume are directly related to the fire characteristic diameter,  $D^*$ , which can be expressed as follows :

$$D^* = \left( \frac{Q}{\rho_0 c_p T_o \sqrt{g}} \right)^{2/5} \quad (9)$$

where  $Q$  is heat release rate (kW),  $\rho_o$  is ambient density ( $\text{kg}/\text{m}^3$ ),  $c_p$  is heat capacity ( $\text{kJ}/(\text{kg}\cdot\text{K})$ ),  $T_o$  is ambient temperature (K),  $g$  is gravitational acceleration ( $\text{m}^2/\text{s}$ ).

It is shown in Eq. (9) that the characteristic diameter  $D^*$  is directly related to the heat release rate. Previous studies show that there will nearly be no difference in the results if the grid sizes are smaller than  $0.075D^*$  to  $0.1D^*$  [34]. The grid size is chosen to be 0.005 m. This means that 20 grid points spans the test sample in one direction. The corresponding heat release rate is around 0.5 kW. Note that a fire increases gradually in the fire growth period, that is, the heat release rate increases from 0 to a certain value. This may indicate that in order to well resolve the fire plume the grid size needs to be infinitely small. This however is not practical. In reality, the computation time is huge for a grid size of 0.005 m and the test duration of 1000 s. In any case, some errors could be introduced due to the difficulty in resolving the fire plume in the growth period.

In the following, cone calorimeter test data and FDS results are compared. Figure 15 shows the comparison of the heat release rate per unit area (HRRPUA) curve obtained from tests and simulations for the floor sample. The curves from the two tests correlate

well with each other, indicating good repeatability. It shows that the simulated results approximately follows the test data and the ignition time is well predicted. However, the simulated heat release rate is much higher after 500 seconds. Clearly, it indicates that energy content consumed in the simulation is higher than that in the test. This could be partly attributed to the uncertainty of the TGA test, e.g. the residue left is too high as the sample was not cut into very fine pieces.

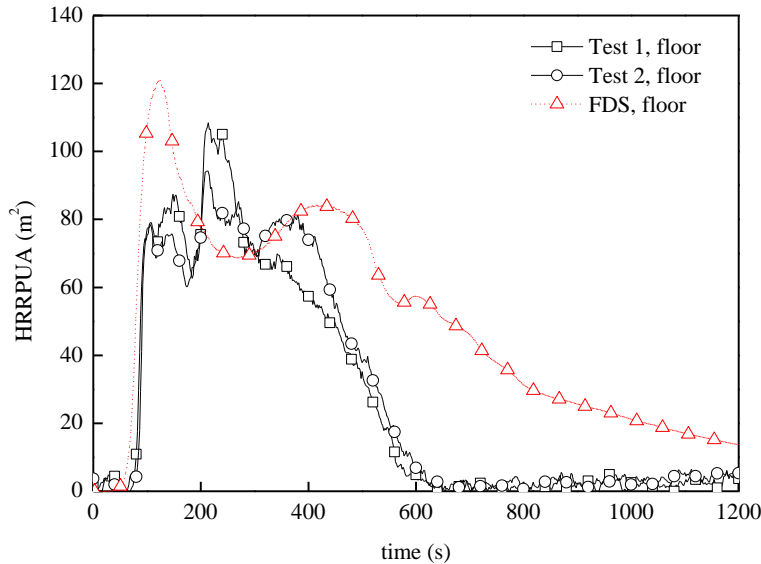


Figure 15 Comparison of heat release rates of the floor sample in cone calorimeter.

Figure 16 shows the comparison of the HRRPUA curve obtained from tests and simulations for the wall sample. Data from the two tests do not correlate very well. It shows that the simulated results approximately follow the test data while the simulated second peak is reached slightly earlier. This could be due to the fact that the low density plastic membrane below the HPL laminate is highly flexible which may affect the burning of the sample.

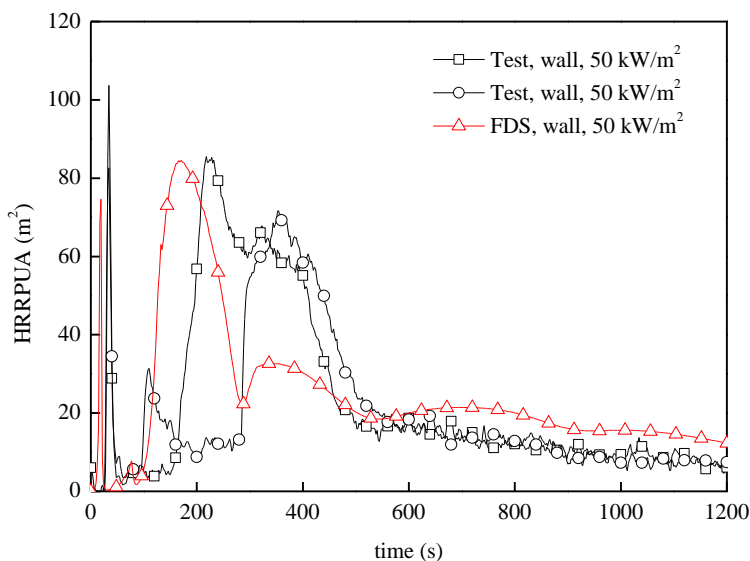
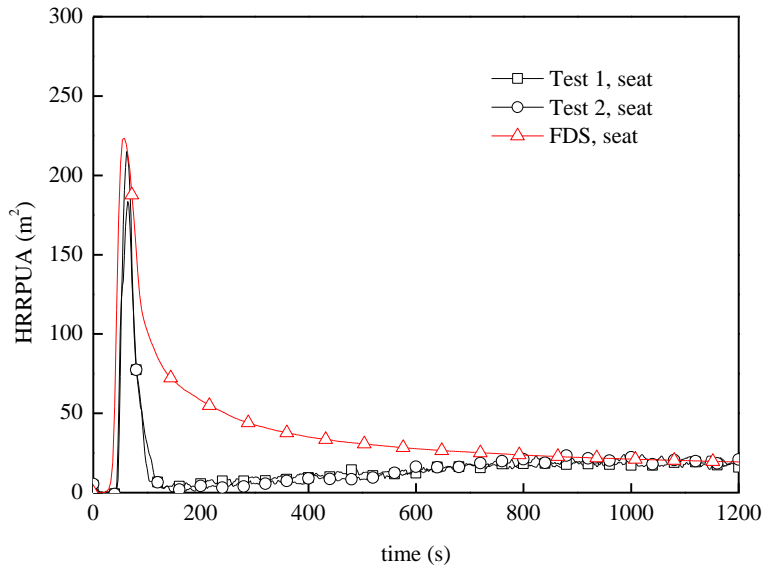


Figure 16 Comparison of heat release rates of the wall sample in cone calorimeter.

Figure 17 shows the comparison of the HRRPUA curve obtained from tests and simulations for the seat sample. Data from the two tests correlate very well with each other. The simulated results correlate well with the test data with the only exception of the overshooting in the decay period.



*Figure 17 Comparison of heat release rates of the seat sample in cone calorimeter.*

Overall, the simulated results correlate with the test data reasonably well. The ignition times for the fuels are predicted well. This indicates that the parameters related to the heat transfer and pyrolysis processes are reasonable.

## 6 CFD modelling of full scale tunnel fire tests

### 6.1 CFD model and parameters

#### 6.1.1 Geometrical model

The full scale tunnel model with the train model is shown in Figure 18. More details of the train model is shown in Figure 19.

The computation domain is 50 m long, 6 m wide and 6.9 m high. In other words, the tunnel is 50 m long by default. The driver cabin is located 10 m downstream of the air flow inlet. The grid size within the train section is 0.1 m. The total number of grid points for the 50 m long tunnel is around 1.2 million.

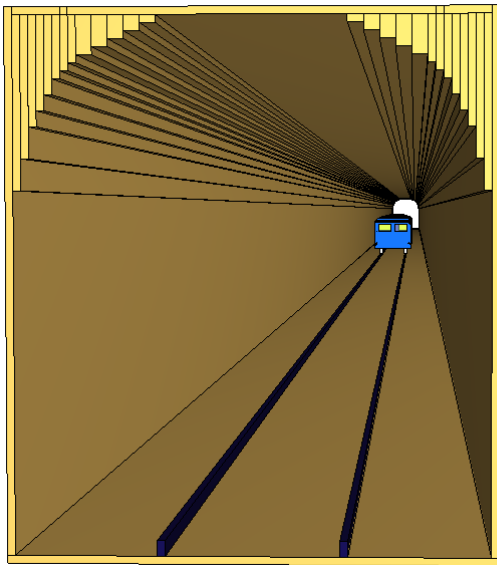


*Figure 18 CFD model of train carriage in the tunnel. The blue one inside the tunnel is the train.*

The train model consists of a 22 m long carriage and a 2.6 long driver cabin. The dimensions are the same as in the full scale test.

Three doors on the bottom side of Figure 19 are open while the other three on the other side are closed at the beginning. However, observations after the tests showed that all the doors fell down. During the test the fall of one door even destroyed some measurement equipment.

The change of openings affects the availability to oxygen in a carriage fire. From previous model scale tests and theoretical studies [30, 35], it has been found that more openings increases the fire spread rate along the carriage and also increases the maximum heat release rate. Therefore, the breakage of the windows and the fall of the doors play a key role in the fire development of the carriage. However, neither of them could be easily estimated. Some assumptions need to be introduced to simulate the realistic scenario as reasonably as possible.

In the modelling, the breakage of the windows, incl. those in the doors, are controlled by gas temperatures beside them. When the gas temperature beside the centre of a window exceeds 600 °C the windows is assumed to break up [1].

A similar assumption is made to the doors that were closed at the beginning. When a gas temperature beside the bottom of a door exceeds 600 °C the door is assumed to fall down due to loss of strength.

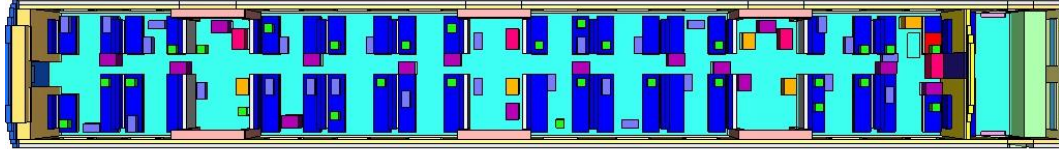


Figure 19 CFD model of train carriage (top view). Red boxes are large luggage. Yellow ones are medium luggage. Purple ones are cabin bags. Lilac ones are sports bag and green ones are backpack.

## 6.1.2 Boundary conditions

The upstream tunnel boundary is set to inlet boundary. The downstream tunnel boundary is set to pressure boundary.

To simulate the full scale test 2, the inlet boundary is forced to approximately follow the velocity curve obtained from the test, see Figure 20.

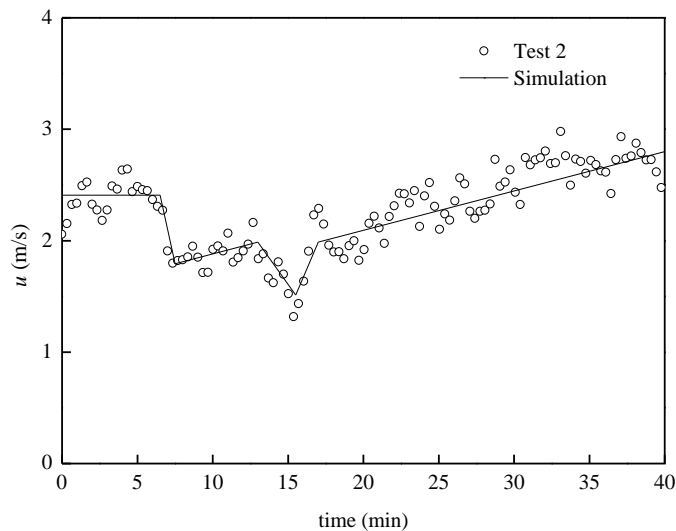


Figure 20 Inlet boundary conditions for the validation simulation.

## 6.1.3 Fuels

The fuels inside the carriage mainly consisted of floor, walls, ceiling, seats and luggage. The metro carriage is made of steel. A thin steel plate with a insulation board behind mostly existed beneath the interior combustible materials.

The fuels on the floor consists of two layers, one with PVC carpet glued onto plywood and the other with styrofoam. The fuels on the walls and the ceiling consisted of two layers, one with HPL laminate and the other with a special polyester insulation. The fuels on the seat consisted of three layers: thin fabric with polyurethane foam, cork wood, and painted wooden board. The properties for the plywood are used for the cork wood and painted wooden board due to lack of information.

Four types of luggage are simulated. A field survey carried out in the METRO project [3] indicates that on average the luggage on the trains consist of approximately 60 % cellulosus material and 40 % plastics. As the fuels placed in luggage are complicated, neither TGA nor cone calorimeter tests was carried out. Instead, single item tests were carried out for all the typical luggage. In these tests, the item was ignited with a burner placed below the item and no external heat flux was imposed on it. This could be very different to a real carriage fire where the unburnt or burning fuels could be exposed to very high external incident radiation from the flames and hot gases nearby. Still, these test data serve as good references in estimation of burning behaviour.

In the CFD modelling, the luggage is simulated with small objects with exposed fuel surfaces, see Table 2. The simple ignition model is applied and the heat release rates are pre-set for each type of luggage. The auto-ignition temperature is set to 500 °C. The reason will be explained later. The maximum heat release rate per unit area is estimated to be approximately 494 kW/m<sup>2</sup> for the luggage consisting of approximately 60 % cellulosus material (108 kW/ m<sup>2</sup> for wood [36]) and 40 % plastics (1072 kW/m<sup>2</sup> for polystyrene [37]). From the data from laboratory tests, it can be found that the HRR reaches the maximum value at around 3 min for all the luggage types. Duration of the decay period and the growth period are assumed to be the same. As an example, the HRR curve for the luggage LA is shown in Figure 10. The luggage starts to burn after the surface temperature reaches the ignition temperature. The heat release rate increases with time in the growth period and reaches the peak at around 3 min. Afterwards the HRR keeps constant and starts to decay at around 600 seconds.

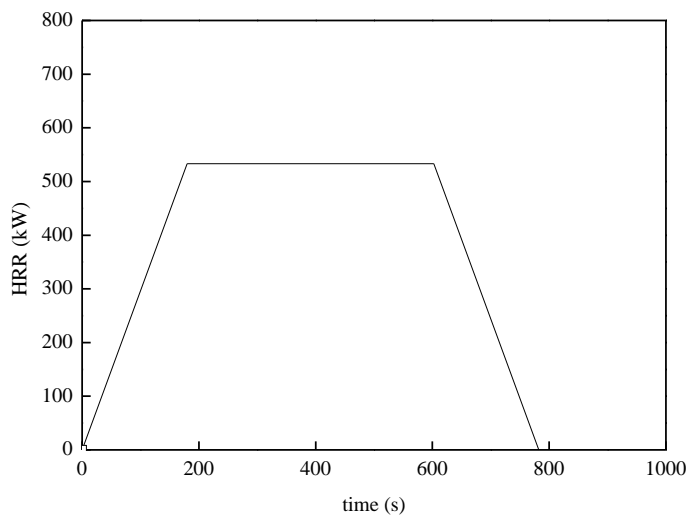


*Figure 21 HRR curve for a single large luggage. The starting time in modelling in fact is controlled by the ignition temperature. There were in total 4 large luggage in the carriage.*

*Table 2 Inputs for the luggage in the carriage.*

Type	Description	Geometry L×W×H	Energy content	HRRmax
		m	MJ	kW
LA	Large luggage	0.4×0.5×0.6	350	534
LB	Medium luggage	0.3×0.4×0.6	250	415
LC	Cabin bag	0.3×0.4×0.6	133	415
LD	Sports bag	0.15×0.25×0.3	75	119
LE	backpack	0.15×0.25×0.35	75	138

The separation wall between the carriage and the driver cabin is combustible and found to burn out after the test. The estimated burn out time for the separation wall is around 40 min after which the windows in the driver cabin broke up and the flames came out.

The ignition source consisted of 1 litre gasoline filled in one common milk package. During the test, some igniters were placed on the seat and the floor beside. The gasoline was then poured to the seat beside the driver cabin and some to the floor, simulating an arson scenario. The gasoline is therefore immediately ignited. The burning area is estimated to be 0.2 m<sup>2</sup> on the seat and 0.36 m<sup>2</sup> on the floor beside the seat. The burning duration is estimated to be around 30 seconds for the gasoline from the observation and the heat release rate per unit area is therefore estimated to be around 1.5 MW/m<sup>2</sup>. The time to reach the peak burning is set to be 10 seconds as the observation showed that burning of the gasoline immediately reaches the steady level after ignition.

Both the pyrolysis model and the simple ignition model are applied to simulate the fire development in the carriage in the full scale tunnel fire test 2.

### **6.1.3.1 Kinetic pyrolysis model**

In simulations with the kinetic pyrolysis model, the pyrolysis properties obtained from cone and TGA are used as inputs for this simulation. Note that the ignition model is still used for the luggage due to the complexity of items inside and also lack of information.

### **6.1.3.2 Simple ignition model**

In simulations with the simple ignition model, the ignition temperature is one of the most important parameter for modelling of fire spread. However, the ignition temperature measured from most laboratory tests in fact cannot directly be used for modelling. The reason is that the ignition temperature varies with the external conditions, e.g. heated by convection or radiation, pilot or auto ignition. For fire spread along the carriage, the key fire spread mechanism that has been identified is the radiation from the upper layer hot gases and neighbouring flames. It can be expected that the main ignition mechanism for most of the fuels are auto-ignition (spontaneous ignition) rather than pilot ignition.

There are very limited data on the critical surface temperature for auto-ignition. However, it is known that for a given fuel the auto-ignition temperature is higher than the pilot ignition temperature. For wood under radiation heating, the auto-ignition temperature is 600 °C, compared to 300-410 °C for pilot ignition [38]. For wood under convective heating, the auto-ignition temperature is 490 °C, compared to 450 °C for pilot ignition [38]. Therefore, for wood, the auto-ignition temperature could lie between 490 °C and 600 °C, and the actual value depends on which mechanism is dominant.

For wood and some typical plastics, the pilot ignition temperature is mainly in a range of 300 °C to 400 °C [32], and the data for wood correlate well with those for plastics. Therefore it may be expected that auto-ignition temperatures for typical plastics could also be close to those for wood. Further, the auto-ignition temperature for flammable gases and vapours could be used as indicators. Test data show that the auto-ignition temperature for flammable gases and vapours is mainly in a range of 400 °C to 600 °C [32]. Note that the temperature difference between the fuel surface and fuel gases within the viscous boundary layer should be limited. Therefore these values reflect the critical surface temperatures for auto-ignition.

The actual fuels burned in the full scale carriage fire test consist of approximately 60 % cellulosic material and 40 % plastics. Based on the above analysis, it is reasonable to assume that for these fuels the auto-ignition temperatures are in a range of 400 °C to 600 °C. An average value of 500 °C is therefore assumed for the fuels. The reason for not choosing the higher value of 600 °C is that some fuels close to each other could be ignited directly by the flame (pilot ignition).

In simulations with the simple ignition model, another important parameter to prescribe is the heat release rate after ignition of a specific fuel. This has to be prescribed for each fuel type. However, the heat release rate curve from cone calorimeter tests cannot directly be used for modelling as the exposed heat fluxes are in reality very different. Test data have to be extrapolated before the possible use for the carriage fire. The smoke temperatures inside the carriage mainly range from 600 °C (responsible for ignition) to 1000 °C (fully developed). The corresponding incident heat fluxes range from 33 kW/m<sup>2</sup> to 150 kW/m<sup>2</sup>. In comparison, the values in the cone calorimeter tests are 25 kW/m<sup>2</sup> and 50 kW/m<sup>2</sup>. Therefore, the heat fluxes in carriage are around 1.3 to 3.0 times that in the cone calorimeter test, with an average value of around 2. Note that the heat release rate is approximately proportional to the heat flux [32]. Based on the cone calorimeter data with low heat fluxes, the maximum heat release rate is therefore chosen to be around 250 kW/m<sup>2</sup> for the floor, 150 kW/m<sup>2</sup> for the wall and ceiling, and 400 kW/m<sup>2</sup> for the seat, respectively. These values correlate well with the values for similar types of fuels in the literature [36] and in our test database. The time between the ignition and maximum heat release rate was set to be the same as in the cone calorimeter tests for individual fuels and the duration of the burning was estimated based on the energy content for each fuel type.

## 6.2 Simulation with simple ignition model

Figure 22 shows a comparison of the simulated heat release rate curve using the simple ignition model and the full scale test data. It can be seen that the simple ignition model predicts the heat release rate well during the whole period with the only exception that the predicted fire growth rate is slightly lower than the test data. The simulated starting time for rapid fire development also complies with the test data.

However, the simulated fire develops slightly slower. This could be due to the fact that for all the fuels, the duration of the fire growth period is assumed to be the same as in the laboratory tests, i.e. the cone calorimeter tests and the luggage tests, where there were either lower or no external heat fluxes. In case that the duration of the fire growth period is shortened the fire should develop more rapidly and the resulting heat release rate could be closer to the test data.

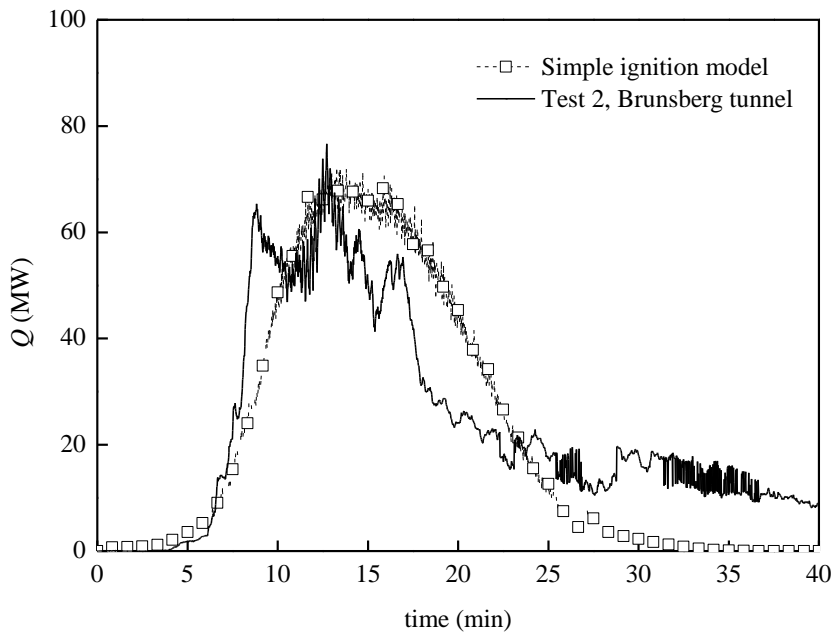


Figure 22 Comparison of test data of HRR in Test 2 and the FDS results with the simple ignition model.

### 6.3 Simulation with kinetic pyrolysis model

Figure 23 shows the simulated heat release rate curve using the kinetic pyrolysis model and the full scale test data. It can be seen that the fire growth simulated correlate well with the test data while the maximum heat release rate is much lower than the test data. Further, the total energy content consumed in the simulation is apparently lower than that in the test.

Some possible reasons are listed here:

1. TGA tests may not produce accurate kinematic parameters: partly due to the fact that the samples were not cut into very fine pieces. Further, the low heating rate in TGA tests and no consideration of solid oxidation in simulations could also have an influence. There could probably be some errors regarding the residue left.
2. Calibration of kinematic parameters based on cone calorimeter data may not be appropriate as the heat fluxes are much lower than in the full scale tests. The heat flux in full scale is in a range of 33-150 kW/m<sup>2</sup> or even higher. This affects the combustion behaviours, e.g. less CO and less soot at the early stage. At later stage, soot and CO may be produced at a large amount inside the carriage but could burn outside the carriage and finally contribute to the total heat release rate. But this is not the case in the cone calorimeter tests. Further, the residue may also be affected by heat fluxes.
3. The energy content is apparently much lower. This somewhat could be attributed to that some other combustible materials such as cables were not accounted for in the simulations.

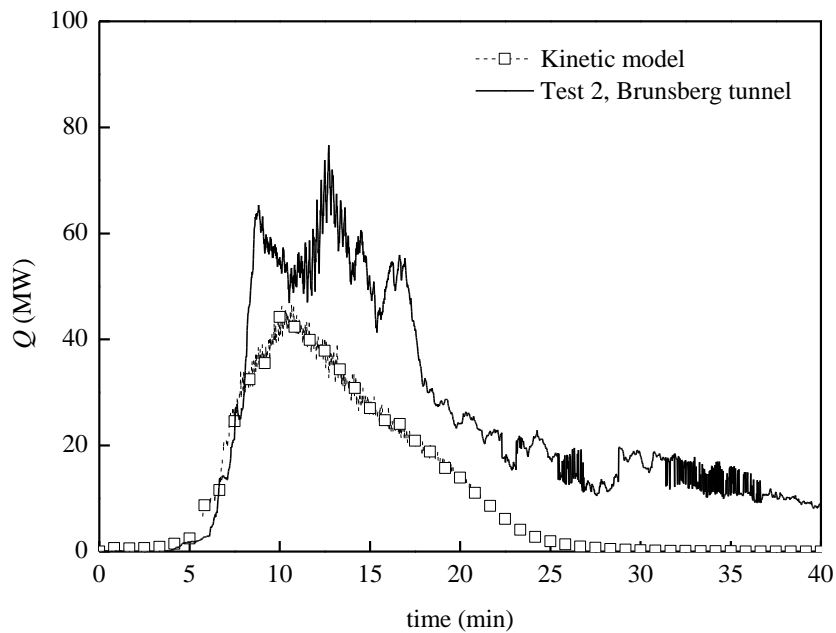


Figure 23 Comparison of test data of HRR in Test 2 and the FDS results with the simple ignition model.

## 6.4 Short summary

Both the simple ignition model and the kinetic pyrolysis model succeed in predicting the fire development in the carriage to some extent. The simple ignition model predicts the heat release rate well during the whole period with the only exception that the predicted fire growth rate is slightly lower than the test data. This could be due to the long growth period estimated from laboratory tests. The maximum heat release rate is predicted well by the simple ignition model.

The kinetic pyrolysis model predicts the growth period well while the maximum heat release rate is lower and the fire decays earlier. It shows that the energy content consumed in the simulation is much lower than that in the test. This could be attributed to the uncertainty related to the TGA tests and cone calorimeter tests and possible fuels that are not accounted for. It is also found that the kinetic pyrolysis model is very sensitive to many parameters, e.g. the residue. Cautions should therefore be taken in practice.

Overall, the simple ignition model could be deemed to perform slightly better than the kinetic pyrolysis model in predicting the fire development in the carriage. However, for any simulation using these pyrolysis models, validation is always required, due to the sensitivity of these pyrolysis models to the input parameters, especially for the kinetic pyrolysis model.

## 7 Effect of ventilation and tunnel structure

### 7.1 Effect of tunnel structure

The train carriage in the open without wind is simulated. The purpose is to investigate the effect of tunnel structure on fire development in the carriage. The tunnel structure could have influence on fire development in the carriage in two main ways: heat feedback from the tunnel structure and ventilation conditions. In this section, only the first effect is discussed. The second effect will be discussed in the following sections.

The simple ignition model is used in this section. The same carriage model is applied but the computation domain is slightly larger to ensure the appropriateness of the open boundaries.

The computation domain is 50 m long, 6 m wide and 9 m high, see Figure 24. From the results, it is known that all fuels are burnt inside the domain. The grid size is 0.1 m. The total number of grids is around 2.7 million.

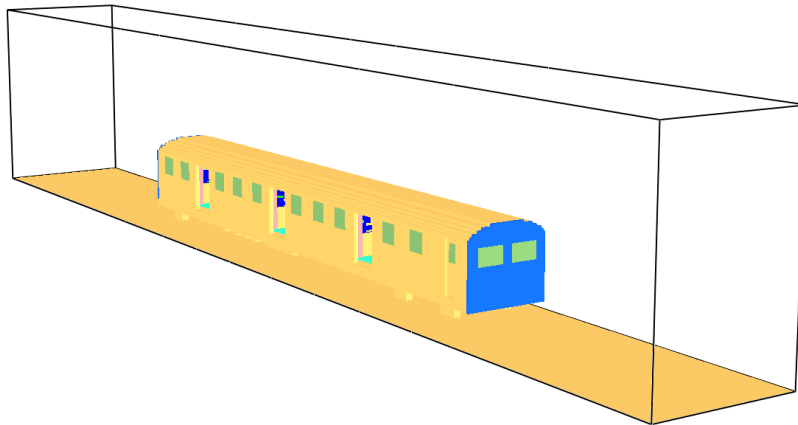


*Figure 24 CFD model of train carriage in the open.*

A comparison of heat release rates of the carriage in the open and in the short tunnel without ventilation is shown in Figure 25. Clearly, they match very well with the only exception that the open fire develops slightly faster. This indicates the effect of tunnel structure (or tunnel walls) nearly has no influence on the fire development or fire spread in the carriage. In other words, the effect of heat feedback from the tunnel structure is negligible for the carriage fires in this short tunnel. Further, this could indicate that the ventilation conditions inside the carriage are not influenced by the tunnel geometry in the simulations.

It is also shown in Figure 25 that there is a good correlation in the maximum heat release rates between the case in the open and the short tunnel case with 0 m/s. The flame shapes in these two cases at around 15 min (corresponding to maximum heat release rates) are shown in Figure 26. Clearly, they show a high similarity, i.e. both with significant volumes of flames existing outside of the carriage. This may indicate that a short tunnel could be considered as a large enclosure that nearly has no influence on the burning of the carriage. In other words, carriage fires in such a short tunnel are well ventilated. This correlation could be used for testing of carriage fires in the future.

Based on studies of wood and plastic crib fires, Li et al. [26] concluded that for well

ventilated solid fuel fires, the maximum HRR increases by approximately 25% relative to a free burn test (fire in the open). This slightly differs from the results found here. The present results show only a very slight increase by around 5 % increase in the maximum HRR. The reason could be that the fire in the carriage is much less sensitive to both heat feedback and tunnel ventilation, compared to the fuels exposed to wind in Li et al.'s tests [26].

It should be reminded that in the simulated case with 0 m/s, the tunnel is very short. If the tunnel is long, the vitiated incoming air flows could affect the burning, which will be discussed in Section 7.3.

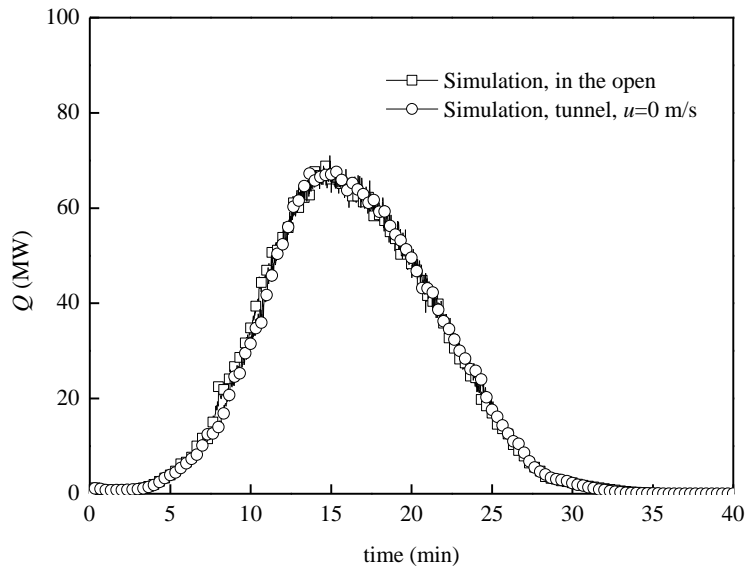


Figure 25 Comparison of heat release rates in the open and in the short tunnel without ventilation ( $u=0$  m/s) with the simple ignition model.

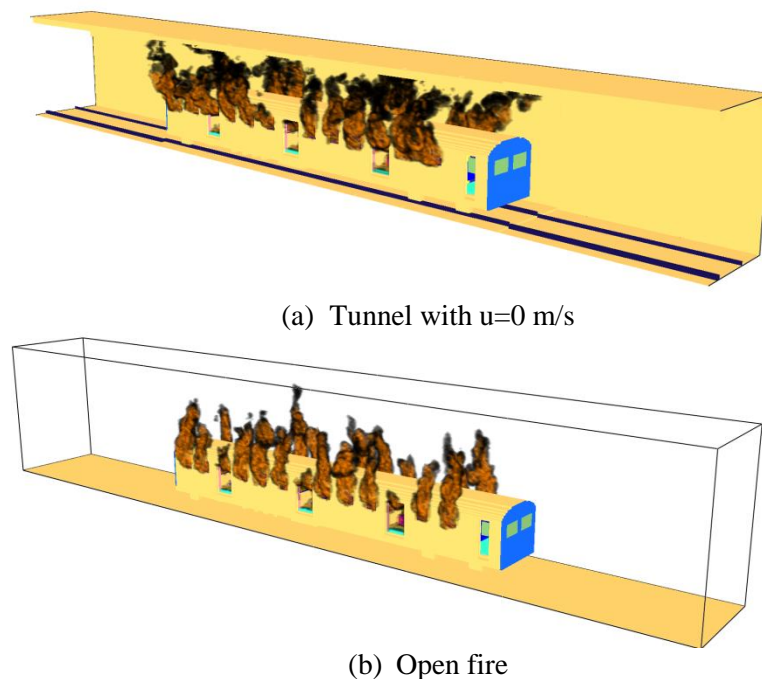


Figure 26 Flame shapes in the open and in the short tunnel without ventilation ( $u=0$  m/s) at around 15 min (simple ignition model).

Note that in the simulation with a velocity of 0 m/s, the tunnel is very short. The effect of tunnel length will be discussed further in the following.

## 7.2 Effect of ventilation in well ventilated fires

The train carriage fires in the tunnel under different ventilation conditions are simulated to investigate the effect of tunnel ventilation on the fire development in the carriage. The cases are divided into two scenarios: well ventilated fires and vitiated fires under low ventilation, based on the effect of tunnel ventilation on the fire development. Both the simple ignition model and the kinetic pyrolysis model are applied.

### 7.2.1 Simple ignition model

The heat release rates simulated with the simple ignition model under different ventilation conditions are shown in Figure 27. The ventilation velocities are 1.5 m/s, 3 m/s and 6 m/s. The simulated results for test 2 are also given. In addition, the short tunnel case with no ventilation ( $u=0$  m/s) is presented for comparison. Under 0 m/s, both tunnel portals were set to open pressure boundary. As mentioned previously, the short tunnel case with 0 m/s could be well ventilated. In the simulated test 2 the velocity is in a range of 1.5 to 2.8 m/s, see Figure 20. In all the simulations, the simple ignition model was applied to simulate the fire development.

Clearly, it shows that the fire develops more rapidly for a higher ventilation velocity but also decays earlier. It also shows that the heat release rate curve in the simulated test 2 lies between the curve for velocity of 1.5 m/s and that for 3 m/s. Note that the velocities in test 2 lie between 1.5 m/s and 3 m/s, and in the linear growth period (between 6.5 min and 11 min) the velocities are mainly in a range of 2 m/s and 2.4 m/s. Further, the maximum heat release rate is insensitive to the ventilation velocity.

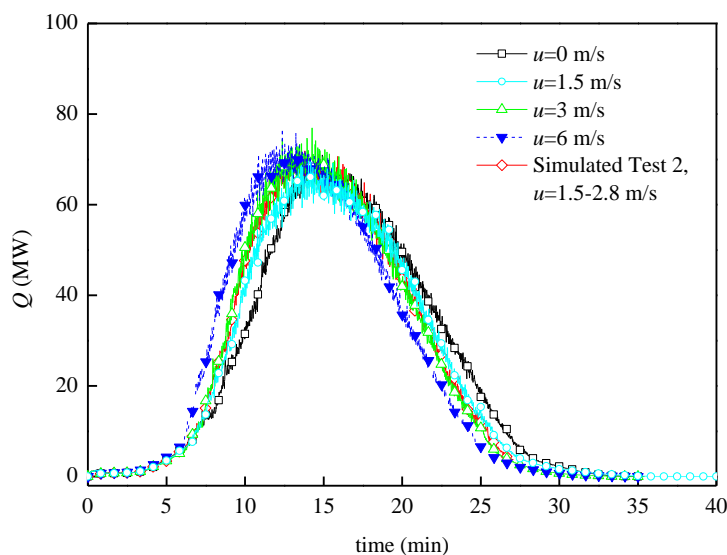


Figure 27 Effect of ventilation on heat release rate for well ventilated fires (Simple ignition model).

## 7.2.2 Kinetic pyrolysis model

The heat release rates simulated with the kinetic pyrolysis model under different ventilation conditions are shown in Figure 28.

It is shown that for a velocity between 3 m/s and 6 m/s, the same trend can be found as in the results with the simple ignition model. The fire develops more rapidly at a higher velocity and also the maximum heat release rate is closely independent of the ventilation velocity.

It is also shown that the simulated heat release rate curve for test 2 is very close to that with 0 m/s. In fact, the fire with 3 m/s develops more rapidly than the case with 0 m/s and the maximum heat release rate is also slightly higher than that with 0 m/s. However, the critical initial fire spread occurs slightly later than that with 0 m/s. This indicates that the ventilation with 3 m/s delays slightly the fire development in comparison to 0 m/s.

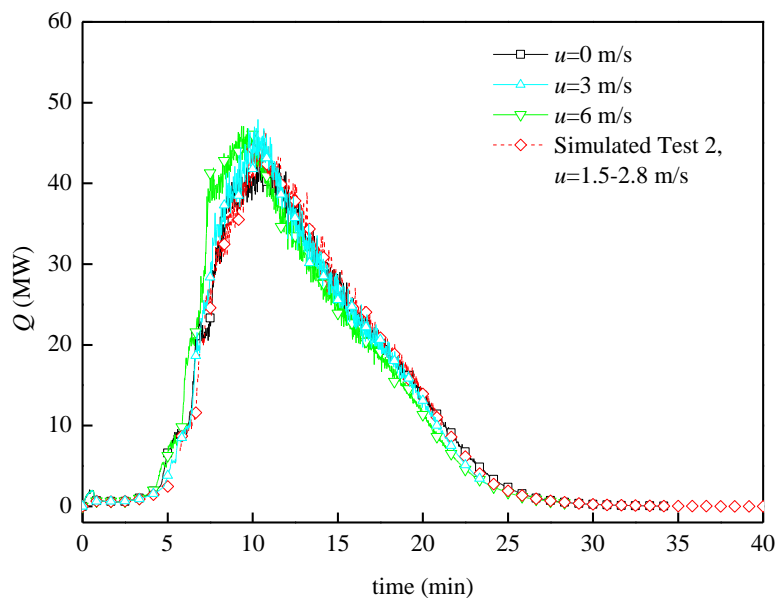


Figure 28 Effect of ventilation on heat release rate for well ventilated fires (kinetic pyrolysis model).

Therefore, for these well ventilated carriage fires, the ventilation has an influence on the fire growth rate, and generally a greater velocity corresponds to a greater fire growth rate, but has very limited influence on the maximum heat release rate.

This correlates well with the findings for fuels exposed to ventilation flows in tunnels. Li and Ingason [27] found that the fire growth rate increases with ventilation velocity based on a theoretical model and a large amount of test data. The test data with 0 m/s however are not considered. Li et al. [26] found that for well ventilated solid fuel fires, the maximum HRR is not sensitive to either tunnel width, tunnel height or ventilation velocity.

## 7.3 Effect of ventilation in vitiated fires under low ventilation

In some cases under low ventilation, significant backlayering could exist [39]. If a tunnel is long, the reverse flow could be blown back to the fire site, resulting in descend of the smoke flow and vitiated incoming air at the fire site. Even if the tunnel is short and most smoke flows out of the tunnel portals, some smoke could still be entrained and blown back to the fire site, which also causes vitiation of the supply air at the fire site. This could significantly affect the combustion behaviours inside the carriage. Here these cases are called vitiated fires under low ventilation.

Vitiation could affect fire development inside the carriage in two different ways. Firstly, the vitiated air with lower oxygen concentration reduces the combustion intensity inside the carriage. This indicates lower radiation heat flux and lower flame spread rate inside the carriage. Secondly, the descend of smoke layer could reduce the thermal pressure difference between the inside and the outside of the carriage, that is, the flow rate could be reduced. In other words, the oxygen supply decreases. In short, the vitiation effect could cause a delay of the fire development and a reduction in the maximum heat release rate. The actual effect depends on the specific ventilation conditions.

### 7.3.1 Heat release rates in vitiated fires

Figure 29 shows the effect of ventilation on the heat release rate in simulations with low ventilation and the simple ignition model. The ventilation velocities are 0 m/s, and 1 m/s. In addition, the case with the ventilation velocity of 3 m/s is presented for comparison. In all the simulations, the simple ignition model was applied to simulate the fire development. It has to be pointed out that by default, inlet boundary conditions are applied, but for simulation with 0 m/s both tunnel boundaries are set to be open pressure boundaries.

It is shown that the heat release rate curve under 0 m/s is very close to those for well-ventilated fires. This indicate that in fact the simulated case under 0 m/s is in fact one well ventilated fire. It should be kept in mind that 0 m/s does not mean that there is no incoming fresh air flow inside the tunnel. Instead the flows are driven by buoyancy, and the incoming fresh air flow balances the outgoing smoke flow. However, note that the tunnel portals are very close to the fire site and both are set to open boundary. If the tunnel is longer and both the upstream section and downstream section are long, the scenario could be very different. This effect will be further discussed in Sect 7.3.3.

It is also shown that the maximum heat release rate is around 45 MW compared to around 70 MW for well-ventilated fires, i.e. 64 % of that for well ventilated fires. This should be due to the effect of vitiation. This phenomenon will be discussed in more detail in the following sections.

Further, the total energy contents consumed in all the simulations are approximately the same due to the fact that the simple ignition model does not account for the interaction between heat feedback and fuel burning rate after a fuel is ignited.

Comparing Figure 29 and Figure 27 indicates that, from the point of view of ventilation effect on the fire development in the carriage, the transition point between the well ventilated fires and vitiated fires lies between 1 m/s and 1.5 m/s.

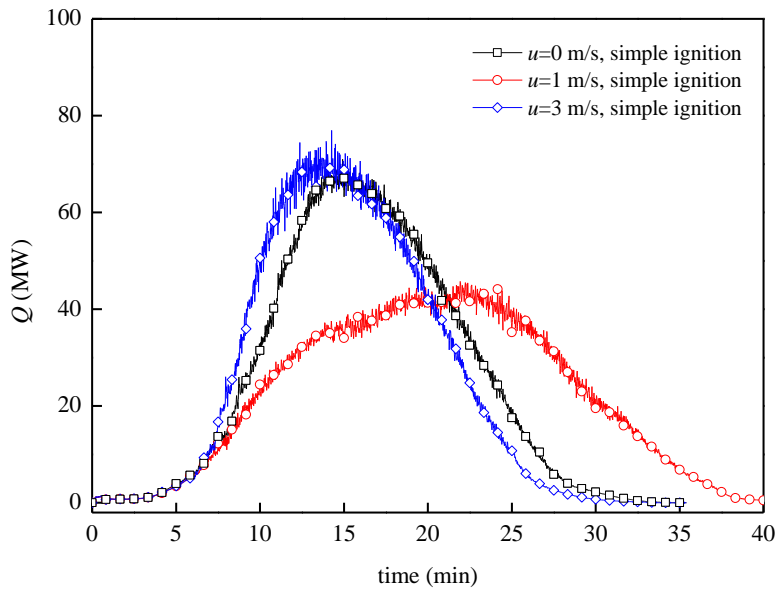


Figure 29 Effect of ventilation on heat release rate for vitiated fires (Simple ignition model).

Figure 30 shows the effect of ventilation on the heat release rate in simulations with low ventilation and the kinetic pyrolysis model. The ventilation velocities are 0 m/s, and 1 m/s. In addition, the case with ventilation velocity of 3 m/s is presented for comparison. In all the simulations, the kinetic pyrolysis model was applied to simulate the fire development. The results are very similar to those with simple ignition model.

It is shown that the maximum heat release rate with 1 m/s is around 24 MW compared to around 45 MW for well-ventilated fires, i.e. 53 % of that for well ventilated fires. The ratio is smaller compared to the simulations with the simple ignition model. This should be due to the effect of lower heat feedback on the fuel burning rate in a vitiated fire which is simulated by the kinetic pyrolysis model but not by the simple ignition model.

It is also shown that the fires develop in a closely same way before 7 min, while after 7 min, the fire with 1 m/s develops much more slowly.

Further, the total energy content consumed with 1 m/s is clearly much lower. This should be due to the interaction between heat feedback and fuel burning rate. It can be expected that the combustion intensity inside the carriage with 1 m/s is much lower than the others.

It is also shown that the fires with 0 m/s and 3 m/s develops in a quite similar way during the whole period. As mentioned previously, the fire with 3 m/s in fact develops little more rapidly and the maximum heat release rate is also slightly higher while the time to reach the critical fire spread occurs little later.

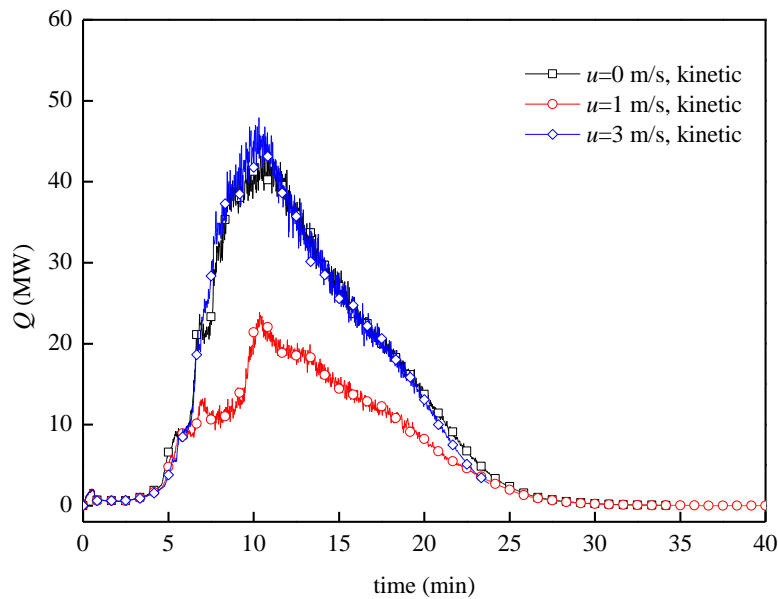


*Figure 30 Effect of ventilation on heat release rate for vitiated fires (Kinetic pyrolysis model).*

In summary, both the ignition model and kinetic pyrolysis models predict slow fire development with 1 m/s after 7 min. Further, the maximum heat release rates with 1 m/s are also lower. This could be due to the vitiation.

Model scale tunnel fire test data [26] showed that for wood and plastic crib fires that were not well ventilated, the HRRs could be less than those in free burn laboratory tests (open fire), and the ratio of the maximum HRR in a vitiated fire to that in a well ventilated fire is around 0.65. In this work this ratio is 0.64 with simple ignition model and 0.53 with kinetic pyrolysis model. Clearly, they correlate relatively well.

The phenomenon of vitiation under low ventilation conditions is further discussed in the following two sections.

### **7.3.2 Vitiation under natural ventilation ( $u=0$ m/s)**

In general, under natural ventilation (no mechanical ventilation), there could still be a dominating flow along the tunnel or a longitudinal flow, in case of a tunnel with a large slope or a fire close to one portal. These cases however are classified as either low ventilation or high ventilation in this work. The natural ventilation here means the case with no dominating flow and the average tunnel velocity is around 0 m/s in the longitudinal direction.

However, a velocity of 0 m/s does not mean that no fresh air goes into the tunnel or no smoke flows out of the fire site. Instead, this case is similar to a compartment fire with an upper hot layer and lower cold layer mostly with no clear distinction. In such cases, the smoke flows outside of the tunnel through both portals where fresh air flows into the tunnel simultaneously. The fresh air could be vitiated as it travels to the fire site. The vitiation effect becomes more severe as the traveling distance increases, that is, when the distances between the fire site and the portals increase.

To analyse the effect of tunnel length and vitiation effect on fire development in the carriage, a simulation with 0 m/s and one 50 m upstream section and one 50 m downstream section was carried out for comparison. The results are compared to the default case, see Figure 31. It is clearly shown that the fire with longer tunnel length develops more slowly after around 12 min. Further, the maximum heat release rate is around 7 MW lower. Therefore the ratio of maximum heat release rate in the longer tunnel to that in the short tunnel is around 0.9. The reason for this reduction can be found in Figure 32 and Figure 33. Clearly, the smoke layer height in the long tunnel is much lower nearby the carriage, i.e. the smoke layer height is close to the window bottoms in the long tunnel while it is close to upper edges of the windows in the short tunnel. The descend of smoke layer indicates vitiated air flows.

Note that in the simulations the scenario in the short tunnel is closely the same as that in the open. Therefore, the ratio of maximum heat release rate in the longer tunnel to that in the open free burn test is also around 0.9. Similar results were found in model scale tests with exposed solid fuels [26]. For fires with natural ventilation ( $u=0$  m/s), the maximum heat release rate in a tunnel with a length of 20 times tunnel height (closely the same as the simulation in this work) and fire source located in the middle is around 90 % of that in the open free-burn test [26].

Clearly, the influence of vitiation in tunnels of such lengths is not significant as rather limited smoke was entrained and blown back to the fire site. It can, however, be expected that if the tunnel becomes longer, the vitiation effect could be more severe, resulting in a much lower fire development and a lower maximum heat release rate.

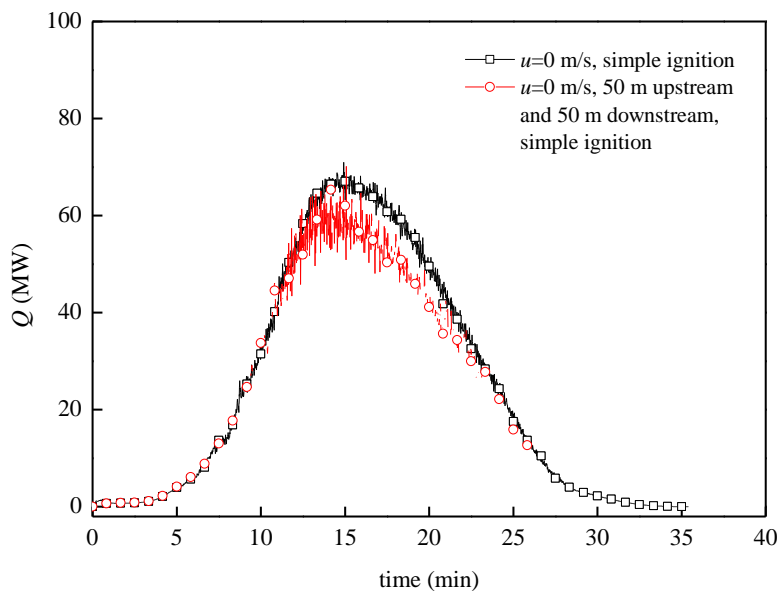


*Figure 31 Effect of tunnel length on fire development under natural ventilation (Simple ignition model).*

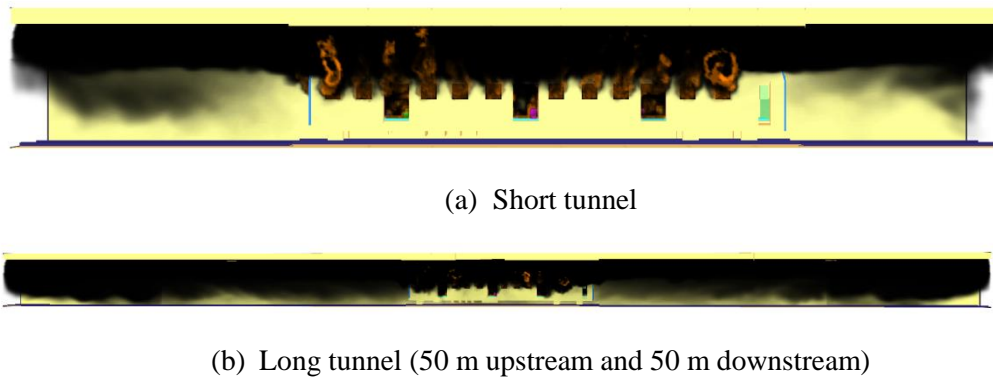


Figure 32 Comparison of smoke distribution in the short and long tunnels at 15 min (Simple ignition model).

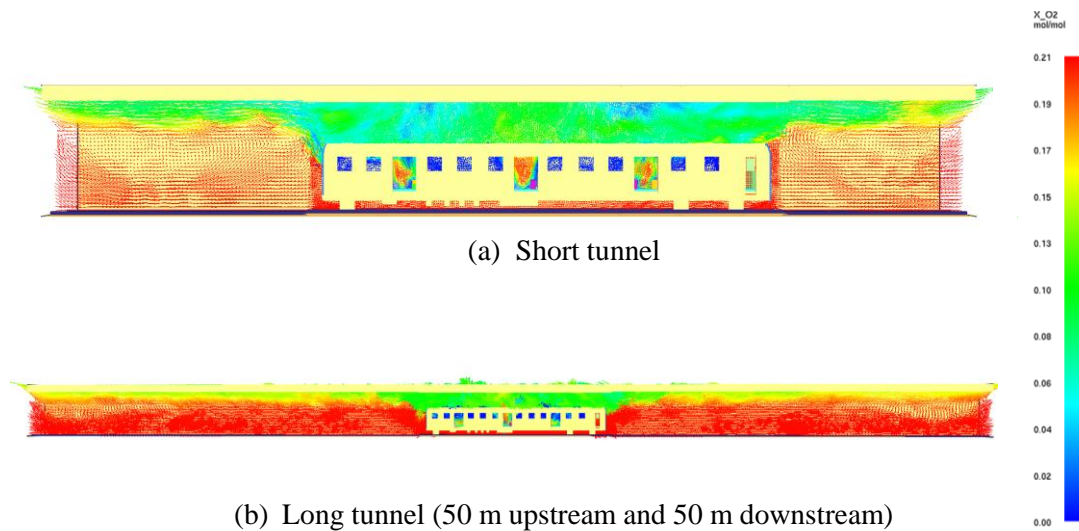


Figure 33 Comparison of oxygen concentration in the short and long tunnels at 15 min (Simple ignition model). The arrow indicates flow direction.

### 7.3.3 Vitiating under low ventilation ( $u=1$ m/s)

If the tunnel under low ventilation is short, the reverse flow could flow out of the upstream tunnel portal. The case is similar to the case with 0 m/s that the smoke flows out on both sides.

If the tunnel under low ventilation is long, there could be two cases. One case is that the reverse flow flows out of the upstream tunnel portal if the ventilation velocity is very low and the backlayering is long enough. This case is also close to the case with 0 m/s. However, it should be noted that during the traveling of the reverse flow, certain smoke flows are entrained by the incoming flows and become part of it. Therefore the incoming flows are vitiating. Another case is that the reverse flow is arrested by the incoming fresh air flow after it travels to a certain position. After that, the reverse flow is blown back to the fire site, although it could take a certain time to return. Therefore, this case is similar to the case with 1 m/s in the simulation (outflow is not allowed at inlet). In both cases with low ventilation, the incoming air flows are vitiating.

The results with 1 m/s are shown Figure 34. For comparison, results with 0 m/s and 3 m/s are also plotted. Clearly, the fire with 1 m/s develops much more slowly and the corresponding maximum heat release rate is much lower than the others.

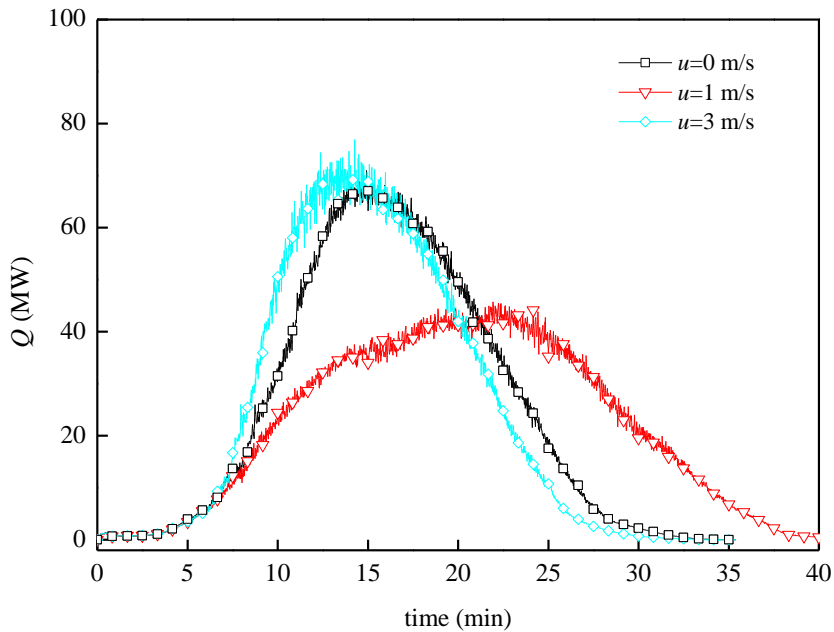


*Figure 34 Effect of ventilation and upstream tunnel length on fire development in vitiated fires with low ventilation (Simple ignition model).*

In the simulations with 1 m/s, the descend of smoke layer in the upstream tunnel section is observed as the backlayering front is arrested by the incoming flow at the inlet boundary. This indicates that the incoming flow at the fire site is vitiated and the oxygen concentration of the incoming air is lower under 1 m/s.

Figure 35 shows a comparison of oxygen concentration for different ventilation conditions at the time corresponding to maximum heat release rate. Under 0 m/s, fresh air flows are induced from both sides and the oxygen level close to the carriage is high. Under 1 m/s, there is some fresh air flow introduced from the left portal, and the oxygen level close to the upstream side of the carriage (right side) is around 17 % (yellow). Under 3 m/s, the fresh air is blown in to the tunnel and no backlayering occurs and thus the oxygen level is high. No flow from left side is introduced. The oxygen concentration in some regions above the carriage with 1 m/s is close to 0, indicating that much fuels are burnt outside the carriage.

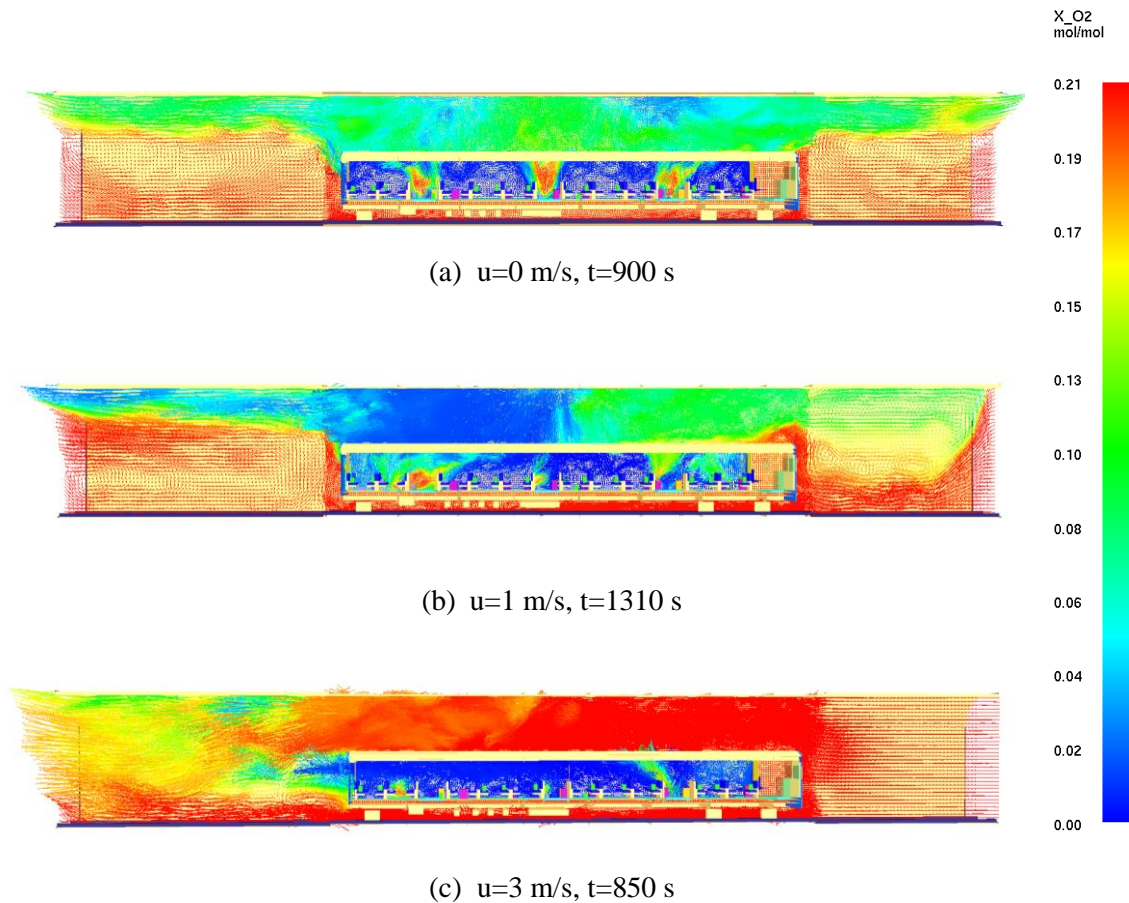


*Figure 35 Effect of ventilation on the oxygen concentration at the maximum heat release rate (Simple ignition model).*

The vitiation under 1 m/s as shown in Figure 35 may be partly due to the upstream section is too short, i.e. inappropriate boundary condition, as outflow is not allowed at the upstream inlet. In the simulations, after the reverse flow reaches the upstream end (the inlet boundary), the smoke reverse flows cannot spread any further and are blown back towards the carriage. This causes the descend of smoke layer and the incoming flow at the fire site is vitiated. In reality, under such conditions with 1 m/s, a significant backlayering exists and length of the backlayering is much longer than the upstream section simulated.

To make the simulations more realistic, two more simulations were carried out with upstream sections of 50 m and 150 m. The results are shown in Figure 36. It is shown in Figure 36 that the heat release rate curves with different upstream tunnel lengths are closely the same. This indicates that the upstream length has only minor effect on the fire development. The de-stratification of the smoke flow upstream of the fire is not attributed to the short upstream tunnel section in the simulation although it is unphysical. Instead, the smoke descend is due to the fact that the backlayering front is arrested by the incoming air flow and all the smoke flow is blown back to the fire site. Therefore, the inflow is highly vitiated, compared to the case with 0 m/s where only a small portion of smoke flow is entrained and blown back to the fire site. Despite this, in the cases with long upstream sections, the heat release rates between 15 min and 27 min are slightly lower than the case with short upstream section, especially for the case with 150 m length between 22 min and 25 min. This indicates that the vitiation effect becomes slightly more severe with increasing upstream length.

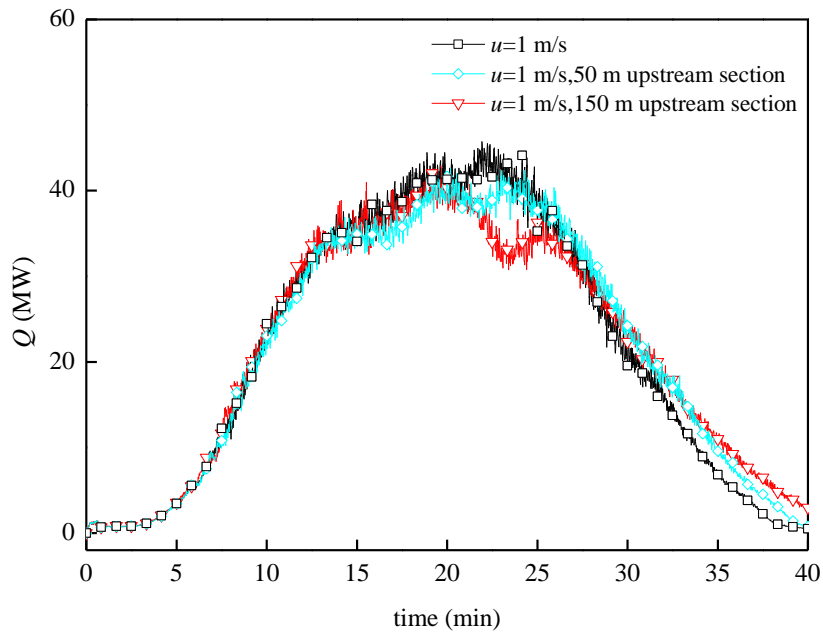
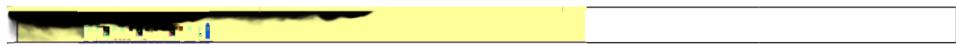


Figure 36 Effect of upstream tunnel length on fire development in vitiated fires with low ventilation (Simple ignition model).

Figure 37 shows the evolution of smoke in the tunnel with 150 m upstream section and 1 m/s. Clearly, the reverse flow moves towards to the right hand boundary (inlet boundary). At 7 min the reverse flow front is at around 30 m upstream of the carriage, and at around 10 min, the smoke front reaches the right boundary (inlet boundary), i.e. 150 m upstream. Therefore the reverse flow move at a speed at around 0.7 m/s in this scenario. During this period, the smoke layer thickness increases continually. Further, after the smoke front is arrested at around 10 min, the reverse flow is blown back and the smoke layer height decreases immediately, similar to a smoke filing process from the right side to the left. At 21 min, the upstream section is full of smoke, similar to the case with 0 m/s (see Figure 32). This also indicates that in fact a significant length of backlayering is not allowed as no smoke stratification will sustain under such conditions.



(a) t=7 min



(b) t=8 min



(c) t=9 min



(d) t=10 min

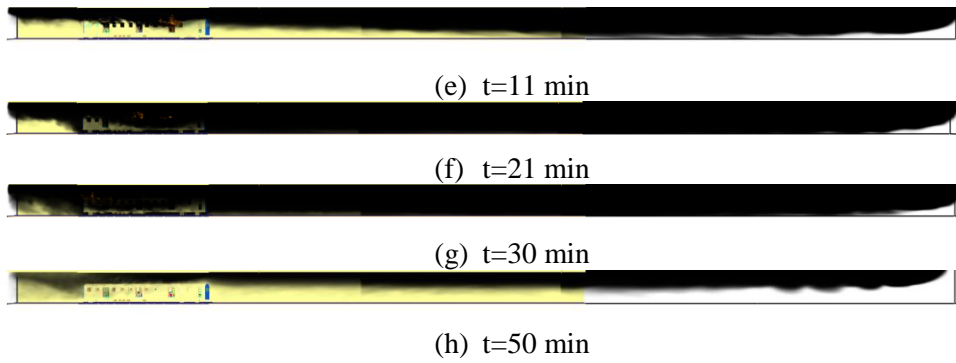


Figure 37 *Evolution of smoke spread in the tunnel with 150 m upstream section and 1 m/s (simple ignition model). Fresh air flows into the tunnel on the right side.*

Figure 38 shows the evolution of Oxygen concentration along the center line of the tunnel with 150 m upstream section and 1 m/s.

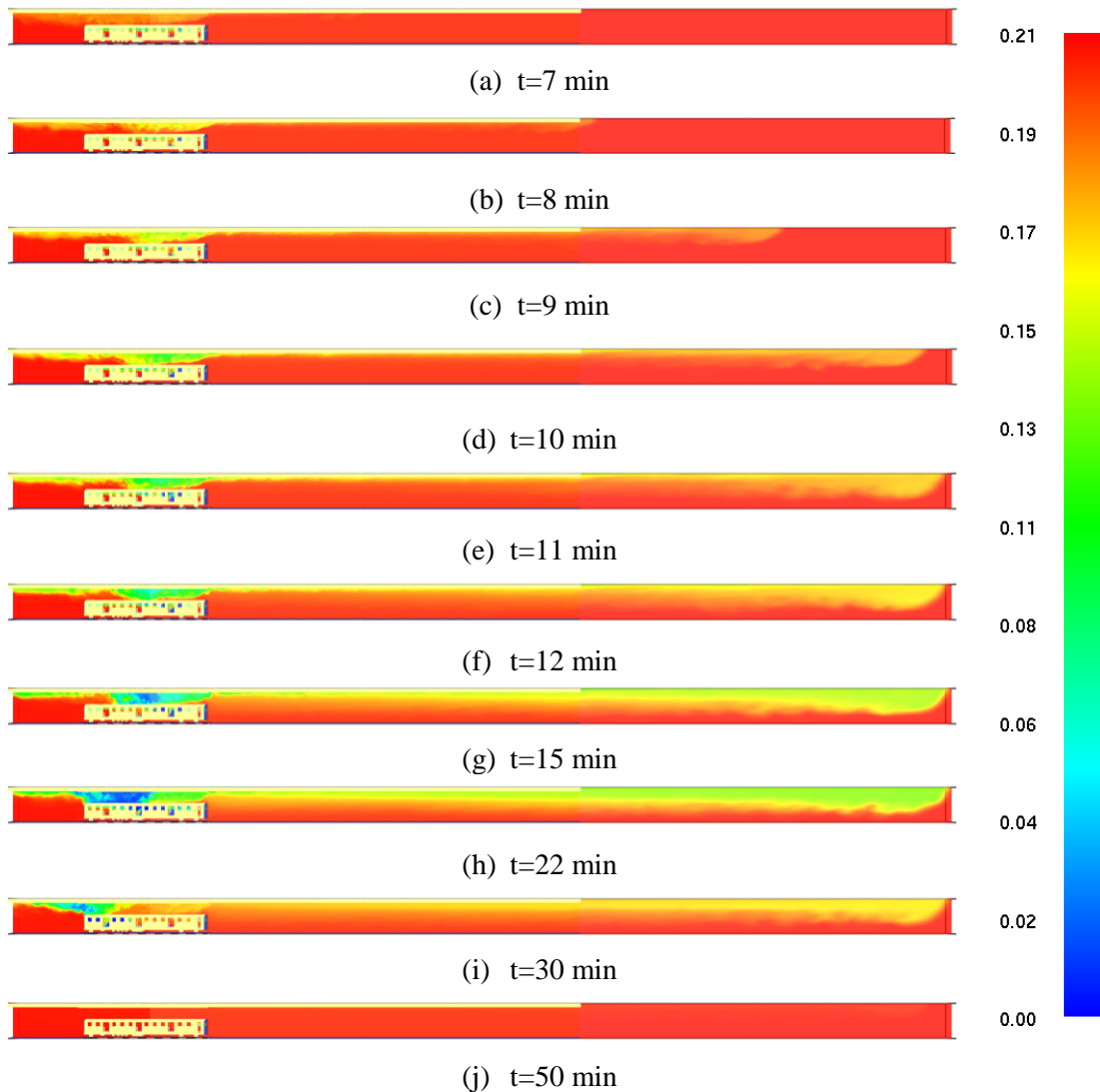


Figure 38 *Evolution of Oxygen concentration in the tunnel with 150 m upstream section and 1 m/s (simple ignition model). Fresh air flows into the tunnel on the right side.*

It is clearly shown in Figure 38 that after the smoke front is arrested at around 10 min, the oxygen concentration nearby the carriage starts to decrease, and it is around 17 % at 22 min. This indicates that the fire is highly vitiated. As the heat release rate decreases after 22 min the oxygen concentration increases with time.

It can be expected that if the fire size is smaller, both the amount of oxygen consumed and the mass flow rate of the reverse flow are less, indicating less significant effect of vitiation on the fire development.

The vitiation can have a major effect on the local combustion behaviours, e.g. lower gas temperatures due to limited oxygen. This lowers the heat feedback from flames and hot gases, which dominates the burning rates of solid and liquid fuels.

## **7.4 Effect of ventilation in closely ventilation controlled fires**

In contrast, in some cases with large fires (fuel rich), the fire could be closely ventilation controlled, that is, the heat release rate is directly related to the fresh air flows that are entrained into the fire site.

For high ventilation, the tunnel flow could be assumed to be one dimensional, and the fresh air flow rate can be easily calculated. In such cases, most of oxygen could be consumed. We may define this parameter as “oxygen efficiency”, i.e. the ratio of the oxygen consumed and the total oxygen available in a tunnel. In other words, the oxygen efficiency could be close to 1 in such cases. Under natural ventilation without wind ( $u=0$  m/s), the fresh airs are induced from both tunnel portals and the rates can be estimated from the classical theory of compartment fires. However, significant vitiation could occur in such cases, depending on the distances between the fire site and the portals. It could therefore be concluded that the oxygen efficiency in such cases could probably be less than that for high ventilation. For low ventilation, if a long smoke backlayering is arrested in a tunnel the fresh air could be highly vitiated and the oxygen efficiency could be lower than the above two cases. From Ingason and Li’s model scale test data with wood crib fires [40], it can be found that the average oxygen efficiency is around 74 % for those vitiated fires (or closely ventilation controlled fires), but close to 1 in some cases.

For the scenarios that are of main interest, e.g. train carriage fires, the fires are mostly not of these types. In other words, most carriage fires in tunnels are fuel controlled despite the fact that inside a carriage the fire could closely be “ventilation controlled” to some extent, i.e. local flashover in some parts of the carriage. Therefore, the above considerations of ventilation controlled fires are not required for most train carriage fires.

## 8 Summary and conclusions

Fire development in a train carriage is investigated by numerical simulations. Two methods, i.e. the simple ignition model and the kinetic pyrolysis model, are applied. The model parameters are estimated and calibrated based on data obtained from TGA tests and cone calorimeter tests.

The first part of the work is to compare the simulated heat release rate curves with data from a full scale carriage fire test. The comparison shows that both the simple ignition model and the kinetic pyrolysis model succeed in predicting the fire development in the carriage to a large extent.

The simple ignition model predicts the heat release rate relatively well during the whole period with the only exception that the predicted fire growth rate is slightly lower than the test data. One possible reason is that the fire growth periods for different fuels were estimated from laboratory tests that could be longer than those in the full scale test where the radiation level inside the carriage is much higher. The maximum heat release rate is predicted well by the simple ignition model.

The kinetic pyrolysis model predicts the growth period well while the maximum heat release rate is much lower and the fire decays earlier. The energy content consumed in the simulation is also much lower than that in the test. These could be due to that some uncertainties could be introduced for the parameters obtained from small scale tests and there could be some fuels that are not accounted for. It is also found that the kinetic pyrolysis model is very sensitive to many parameters.

Overall, the simple ignition model could be deemed to perform better than the kinetic pyrolysis model in predicting the fire development in the carriage. However, for any simulation using these pyrolysis models, validation is always required, due to the sensitivity of these pyrolysis models to the input parameters, especially for the kinetic pyrolysis model.

The second part of the work is to investigate the effects of ventilation and tunnel structure on fire development in carriages.

The results show that for well ventilated carriage fires, e.g. when the longitudinal ventilation velocity is greater than around 1.5 m/s, the tunnel structure nearly has no effect on fire development in the carriage. The fire growth rate increases with ventilation while the maximum heat release rate is closely independent of the ventilation. For carriage fires under such conditions, the maximum heat release rate is approximately the same as that in a free-burn fire test in the open.

When the longitudinal ventilation velocity is not greater than a certain value (e.g. 1 m/s) and the reverse flow is arrested by the incoming flow (e.g. in a long tunnel), the fire could be highly vitiated. The fire develops more slowly and the maximum heat release rate becomes lower. We may call these fires as highly vitiated fires. For carriage fires under such conditions, the ratio of the maximum heat release rate to that in a well ventilated fire (or a free burn open fire) is around 0.6. The main reason should be that under such conditions, there exists a long backlayering with a large amount of smoke, which is prevented by the incoming air flow and then blown back to the fire site, causing immediate smoke descend and vitiation of the fresh air at the fire site.

From the point of view of ventilation effect on the fire development, the distinction between the well ventilated fires and highly vitiated fires lies between 1 m/s and 1.5 m/s.

However, when the reverse flow is not arrested by the incoming flow in a tunnel, e.g. for a short tunnel or for a tunnel with no dominating ventilation (closely 0 m/s), the smoke could flow out of the tunnel through both portals. Under such conditions, there could be only a small portion of smoke is entrained into the incoming flow and blown back to the fire site. We may call these fires as lightly vitiated fires. The vitiation effect, therefore, depends on the tunnel length and the fire location relative to the portals. For a carriage fire in the middle of an approximately 100 m long tunnel, the ratio of the maximum heat release rate to that in a well ventilated fire (or a free burn open fire) is around 0.9. This ratio is expected to be slightly lower for a longer tunnel, but could not be lower than 0.6 which corresponds to highly vitiated fires.

If the fire size is smaller, both the amount of oxygen consumed and the mass flow rate of the reverse flow are less, which indicates less significant effect of vitiation on the fire development. Under such conditions, the distinction point between well ventilated and vitiated fires could also be lower.

For all the cases, the effect of tunnel walls nearly has no effect on fire development in the carriage. Therefore the effect of heat feedback from tunnel structure is negligible for carriage fires. This is mainly due to the fact that the fuels in a carriage are not directly exposed to the tunnel structure.

It should be kept in mind that all the carriage fires discussed in this work are fuel controlled, despite the fact that inside the carriage the fire could closely be ventilation controlled to some extent, i.e. local flashover. In contrast, some large fires, e.g. tanker fires, could be closely ventilation controlled (fuel rich), that is, the heat release rate is directly related to the fresh air flows that are entrained into the fire site.

## References

1. Li YZ, Ingason H, *A new methodology of design fires for train carriages based on exponential curve method*. Fire Technology, 2015.
2. *NFPA 502 - Standard for Road Tunnels, Bridges, and Other Limited Access Highways*, National Fire Protection Association. 2011 Edition.
3. Lönnermark A, Lindström J, Li YZ, Claesson A, Kumm M, Ingason H, *Full-scale fire tests with a commuter train in a tunnel*, in *SP Report 2012:05SP* Technical Research Institute of Sweden: Borås, Sweden. 2012.
4. Carvel RO, Beard AN, Jowitt PW, Drysdale DD, *Variation of Heat Release Rate with Forced Longitudinal Ventilation for Vehicle Fires in Tunnels*. Fire Safety Journal, 2001. **36**(6): p. 569-596.
5. Carvel RO, Drysdale DD, *The Influence of Tunnel Geometry and Ventilation on the Heat Release Rate of a Fire*. Fire Technology, 2004. **40**: p. 5-26.
6. McGrattan K, Hostikka S, McDermott R, Floyd J, Weinschenk C, Overholt K, *Fire Dynamics Simulator Technical Reference Guide Volume 1: Mathematical Model (Version 6)* National Institute of Standards and Technology: USA. 2013.
7. McGrattan K, Hostikka S, McDermott R, Floyd J, Weinschenk C, Overholt K, *Fire Dynamics Simulator User's Guide (Version 6)* National Institute of Standards and Technology: USA. 2015.
8. Ma T.G., Quintierre J.G., *Numerical Simulation of Axi-Symmetric Fire Plumes: Accuracy and Limitations*. Fire Safety Journal, 2003. **38**(5): p. 467-492.
9. Li Y.Z., Ingason H., Lönnermark A. *Numerical simulation of Runehamar tunnel fire tests*. in *6th International Conference on Tunnel safety and Ventilation*. Graz, Austria. 2012.
10. Hamins A, Maranghides A, McGrattan KB, Ohlemiller TJ, Anleitner RL, *Federal Building and Fire Safety Investigation of the World Trade Centre Disaster: Experiments and Modelilng of Multiple Workstations Burning in a Compartment. NIST NCSTAR 1-5E*, National Institute of Standards and Technology: Washington U.S. 2005.
11. Parker WJ. *Prediction of the heat release rate of wood*. in *Proceedings of the first International Symposium on Fire Safety Science*. IAFSS. 1985.
12. Atreya A, *Pyrolysis, ignition and fire spread on horizontal surfaces of wood*, Harvard University. 1983.
13. Chaos M, Khan MM, Krishnamoorthy N, Ris Jld, Dorofeev SB. *Evaluation of optimization schemes and determination of solid fuel properties for CFD fire models using bench-scale pyrolysis tests*. in *Proceedings of the Combustion Institute 33*. 2011.
14. Pau DSW, Fleischmann CM, Spearpoint MJ, Li KY, *Determination of kinetic properties of polyurethane foam decomposition for pyrolysis modelling*. Journal of Fire Sciences, 2013. **31**(4): p. 356-384.
15. Matala A, Lautenberger C, Hostikka S, *Generalized direct method for pyrolysis kinetic parameter estimation and comparison to existing methods*. Journal of Fire Science, 2012. **30**(4): p. 339-356.
16. Rein G, Lautenberger C, Fernandez-Pello AC, Torero JL, Urban DL, *Application of genetic algorithms and thermogravimetry to determine the kinetics of polyurethane foam in smoldering combustion*. Combustion and Flame, 2006. **146**(1-2): p. 95-108.
17. Matala A, Hostikka S, Mangs J. *Estimation of Pyrolysis Model Parameters for Solid Materials Using Thermogravimetric Data*. in *9th International Symposium on Fire Safety Science*. Karlsruhe, Germany: IAFSS. 2008.
18. Lautenberger C, Fernandez-Pello C. *Optimization algorithms for material pyrolysis property estimation*. in *10th International Symposium on Fire Safety Science (IAFSS)*. Maryland, USA. 2011.

19. Kit CM, *Assessment of vehicle fire development in road tunnels for smoke control ventilation design*, PhD thesis, University of Canterbury: New Zealand. 2009.
20. Ingason H, Li YZ, Lönnermark A, *Runehamar Tunnel Fire Tests*. Fire Safety Journal, 2015. **71**: p. 134–149.
21. White N, *Fire Development in Passenger Trains - Master Thesis*, Victoria University, Australia. 2009.
22. Hjohlman M, Försth M, Axelsson J, *Design fore for a train compartment*, SP Technical Research Institute of Sweden: Borås, Sweden. 2009.
23. Guillaume E, Camillo A, Rogaume T, *Application and Limitations of a Method Based on Pyrolysis Models to Simulate Railway Rolling Stock Fire Scenarios*. Fire Technology, 2014. **50**: p. 317–348.
24. Ingason H, Li YZ, *Model scale tunnel fire tests with longitudinal ventilation*. Fire Safety Journal, 2010. **45**: p. 371-384.
25. Ingason H, Li YZ, *Model scale tunnel fire tests with point extraction ventilation*. Journal of Fire Protection Engineering, 2011. **21**(1): p. 5-36.
26. Li YZ, Fan CG, Ingason H, Lönnermark A, Ji J, *Effect of cross section and ventilation on heat release rates in tunnel fires*. Tunnelling and Underground Space Technology, 2015, <http://dx.doi.org/10.1016/j.tust.2015.09.007>.
27. Li YZ, Ingason H. *The fire growth rate in a ventilated tunnel fire*. in *10th International Symposium on Fire Safety Science (IAFSS)*. Maryland, USA. 2011.
28. McGrattan K, Hostikka S, McDermott R, Floyd J, Weinschenk C, Overholt K, *Fire Dynamics Simulator Technical Reference Guide: Volume 2: Verification*, National Institute of Standards and Technology. 2015.
29. ISO, *Reaction-to-fire tests - Heat release, smoke production and mass loss rate - Part 1: Heat release rate (cone calorimeter method)*, ISO. 2002.
30. Lönnermark A, Lindström J, Li YZ. *Model Scale Metro Carriage Fire Tests - Influence of Material and Fire Load*. in *Second International Conference on Fires in Vehicles*. Chicago, USA: SP Technical Research Institute of Sweden. 2012.
31. DiNenno PJ, *SFPE Handbook of Fire Protection Engineering*, Quincy, MA, USA: National Fire Protection Association. 2002.
32. Drysdale D, *An Introduction to Fire Dynamics*. 3rd Edition ed: John Wiley & Sons. 2011.
33. J.G. Q, *Fundamentals of Fire Phenomena*, Chichester, England: John Wiley & Sons Ltd. 2006.
34. Li YZ, Lei B, Ingason H, *Scale modeling and numerical simulation of smoke control for rescue stations in long railway tunnels*. Journal of Fire Protection Engineering, 2012. **22**(2): p. 101-131.
35. Li YZ, Ingason H, Lönnermark A. *Fire development in different scales of train carriages*. in *11th International Symposium on Fire Safety Science*. Christchurch, New Zealand. 2014.
36. Ingason H, Li YZ, Lönnermark A, *Tunnel Fire Dynamics*, New York: Springer. 2015.
37. Tewarson A, *Generation of Heat and Chemical Compounds in Fires*, in *The SFPE Handbook of Fire Protection Engineering*, PJ DiNenno, et al., Editors. National Fire Protection Association: Quincy, MA, USA. 2002, p. 3-82 -- 3-161.
38. Kanury AM, *Ignition of cellulosic materials: a review*. Fire Research Abstracts and Reviews, 1972. **14**: p. 24–52.
39. Li YZ, Lei B, Ingason H, *Study of critical velocity and backlayering length in longitudinally ventilated tunnel fires*. Fire Safety Journal, 2010. **45**: p. 361-370.
40. Ingason H, Li YZ, *Model Scale Tunnel Fire Tests with Point Extraction Ventilation*. Journal of Fire Protection Engineering, 2011. **21**(1): p. 5–36.
41. CEN, *Reaction to fire tests for building products - Building products excluding flooring exposed to the thermal attack by a single burning item*, CEN European Committee for Standardization. 2002.

## Appendix A - Yields of CO and smoke particles

Yields of CO and smoke particles affects the actual heat released into the gas domain, and also affects the radiation transfer and smoke quantities. In FDS simulations, these two parameters are important inputs that have to be pre-defined. In this section, data from cone calorimeter tests are applied to estimate these two parameters.

The CO yield,  $Y_{CO}$  (kg/kg), could be estimated according to the following equation in terms of mass flow rate:

$$Y_{CO}(t) = \frac{\dot{m}_{CO}(t)}{\dot{m}_f(t)} \quad (10)$$

where  $\dot{m}$  is mass flow rate. Subscript CO indicates carbon monoxide and f is fuel.

The CO yield could also be estimated in terms of mass:

$$Y_{CO} = \frac{m_{CO}}{m_f} \quad (11)$$

where  $m$  is fuel mass. Note that this mass corresponds to mass of fuels evaporated, rather than the initial fuel mass.

The soot yield,  $Y_s$  (kg/kg), could be estimated according to the following equation in terms of mass flow rate:

$$Y_s(t) = \frac{SPR(t)}{\sigma_s \dot{m}_f(t)} \quad (12)$$

where  $\sigma_s$  is a specific extinction area ( $9600 \pm 300 \text{ m}^2/\text{kg}$  [41]),  $SPR$  is the smoke production rate parameter ( $\text{m}^2/\text{s}$ ), which is a standard output of one cone calorimeter therefore not discussed further.

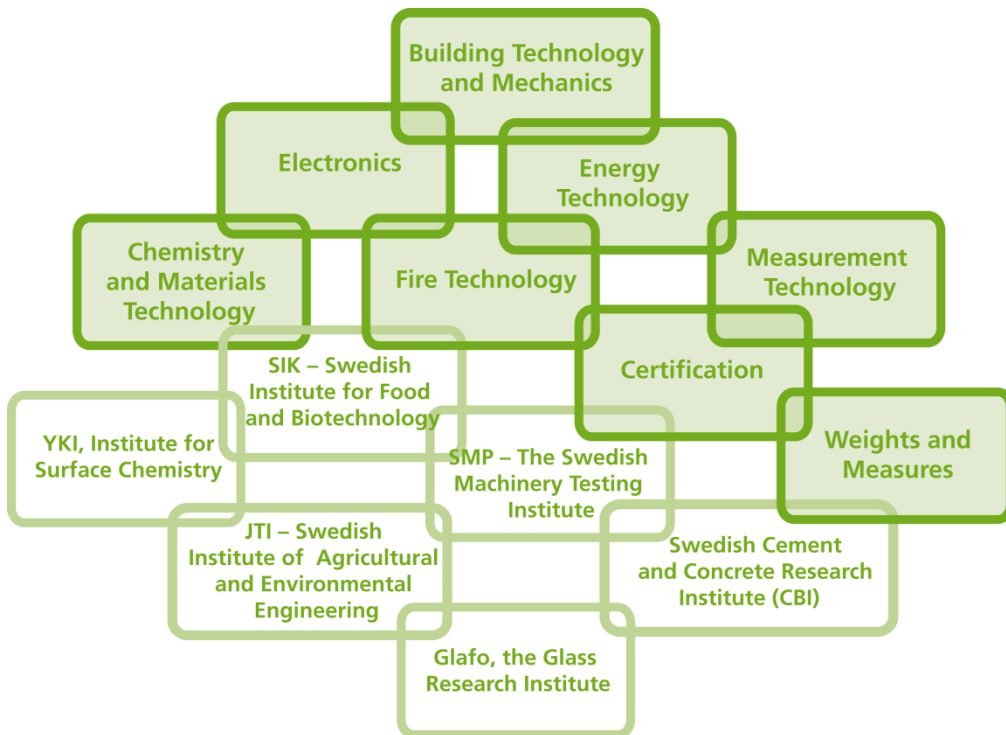
The soot yield could also be estimated in terms of mass:

$$Y_s(t) = \frac{\int SPR(t)dt}{\sigma_s m_f} \quad (13)$$

It should always be kept in mind that estimation of yields of CO and smoke particles are based on the burnt fuel.

### SP Technical Research Institute of Sweden

Our work is concentrated on innovation and the development of value-adding technology. Using Sweden's most extensive and advanced resources for technical evaluation, measurement technology, research and development, we make an important contribution to the competitiveness and sustainable development of industry. Research is carried out in close conjunction with universities and institutes of technology, to the benefit of a customer base of about 9000 organisations, ranging from start-up companies developing new technologies or new ideas to international groups.



### SP Technical Research Institute of Sweden

Box 857, SE-501 15 BORÅS, SWEDEN

Telephone: +46 10 516 50 00, Telefax: +46 33 13 55 02

E-mail: [info@sp.se](mailto:info@sp.se), Internet: [www.sp.se](http://www.sp.se)

[www.sp.se](http://www.sp.se)

Fire Research

SP Report 2015:86

ISBN 978-91-88349-05-7

ISSN 0284-5172

More information about publications published by SP: [www.sp.se/publ](http://www.sp.se/publ)